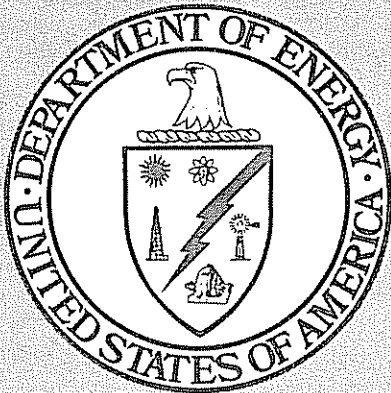


DOE/MC/08216-1354



DOE/MC/08216-1354
(DE83007271)

**MODELING OF DEVONIAN SHALE GAS
RESERVOIRS**

(Conduct Reservoir Modeling for the Devonian Shales)

Final Report

September 1979

Work Performed Under Contract No. AM21-78MC08216

For
Morgantown Energy Technology Center
Morgantown, West Virginia

By
Science Applications, Inc.
Morgantown, West Virginia

TECHNICAL INFORMATION CENTER
UNITED STATES DEPARTMENT OF ENERGY

DISCLAIMER

"This report was prepared as an account of work sponsored by an agency of the United States Government. Neither the United States Government nor any agency thereof, nor any of their employees, makes any warranty, express or implied, or assumes any legal liability or responsibility for the accuracy, completeness, or usefulness of any information, apparatus, product, or process disclosed, or represents that its use would not infringe privately owned rights. Reference herein to any specific commercial product, process, or service by trade name, trademark, manufacturer, or otherwise, does not necessarily constitute or imply its endorsement, recommendation, or favoring by the United States Government or any agency thereof. The views and opinions of authors expressed herein do not necessarily state or reflect those of the United States Government or any agency thereof."

This report has been reproduced directly from the best available copy.

Available from the National Technical Information Service, U. S. Department of Commerce, Springfield, Virginia 22161.

Price: Printed Copy A05
Microfiche A01

Codes are used for pricing all publications. The code is determined by the number of pages in the publication. Information pertaining to the pricing codes can be found in the current issues of the following publications, which are generally available in most libraries: *Energy Research Abstracts, (ERA)*; *Government Reports Announcements and Index (GRA and I)*; *Scientific and Technical Abstract Reports (STAR)*, and publication, NTIS-PR-360 available from (NTIS) at the above address.

FINAL REPORT
MODELING OF DEVONIAN SHALE GAS RESERVOIRS
(Conduct Reservoir Modeling for the Devonian Shales)

BY

Science Applications, Inc.
Suite 8
Chestnut Ridge Professional Building
Morgantown, West Virginia 26505

September 1979

Prepared For

United States Department of Energy
Morgantown Energy Technology Center
Morgantown, West Virginia

Under Contract No. DE-AT21-78MC08216

TABLE OF CONTENTS

| <u>Section</u> | <u>Page</u> |
|--|-------------|
| 1. Summary and Conclusions. | 1 |
| 2. Recommendations. | 3 |
| 3. Introduction | 4 |
| 4. Mathematical Model | 6 |
| 5. Analytical Solutions | 10 |
| 6. Numerical Solutions. | 16 |
| 7. Reservoir-Input Parameters | 19 |
| 8. Results of Sensitivity Analysis. | 22 |
| Nomenclature | 29 |
| References | 30 |
| Appendix A: Development of Flow Model for Devonian. Shale Reservoirs. | 32 |
| Appendix B: Analytical Procedures | 37 |
| Appendix C: Numerical Procedures. | 40 |
| Appendix D: User Procedure and Program Listing. | 46 |
| Table:1: Model Input Data For Sensitivity Analysis. | 76 |

LIST OF FIGURES

| <u>Figure</u> | | <u>Page</u> |
|---------------|---|-------------|
| 1 | - Methane Sorption Isotherms at 28 ⁰ C. | 77 |
| 2 | - Fractured Devonian Shale Reservoir Systems. | 77 |
| 3 | - Radial One-Dimensional Devonian Shale Reservoir Model | 78 |
| 4 | - Reservoir Finite-Difference Grid System | 78 |
| 5 | - Block-Centered Finite-Difference Scheme at the Wellbore | 79 |
| 6 | - Matrix Element Finite - Difference Scheme | 79 |
| 7 | - Damaged Zone in Finite-Difference Scheme. | 80 |
| 8 | - Fracture Permeability versus Fracture Spacing for Various Fracture Widths | 80 |
| 9 | - Comparison of Numerical and Analytical Solutions. | 81 |
| 10 | - Productivity Improvement with Dual Porosity and Desorption. | 81 |
| 11 | - Effect of Fracture Permeability on Cumulative Production. | 82 |
| 12 | - Cumulative Production as a Function of Time for Various Matrix Permeabilities | 82 |
| 13 | - Effects of Fracture Porosity on Cumulative Production | 83 |
| 14 | - Effects of Matrix Porosity on Cumulative Production | 83 |
| 15 | - Comparison of Cumulative Production for Different Matrix Element Sizes | 84 |
| 16 | - Cumulative Production for Different Fracture Permeabilities | 84 |
| 17 | - Production Rate for Different Fracture Permeabilities. | 85 |
| 18 | - Effect of Gas Slippage on Production Rate | 85 |
| 19 | - Breakdown of Resource Recovery. | 86 |
| 20 | - Sensitivity of Various Parameters on Cumulative Production. | 86 |
| 21 | - Comparison of Cumulative Production Using Different Models. | 87 |

1. SUMMARY AND CONCLUSIONS

The Department of Energy (DOE), Morgantown Energy and Technology Center (METC) has been supporting the development of flow models for Devonian Shale gas reservoirs. The broad objectives of this modeling program have been:

1. To develop and validate a mathematical model which describes gas flow through Devonian Shales.
2. To analyze the sensitive parameters that affect the deliverability and recovery of gas from shales.
3. To recommend laboratory and field measurements for determination of those parameters critical to the productivity and timely recovery of gas from the Devonian Shales.
4. To analyze pressure and rate transient data from observation and production gas wells to determine reservoir parameters, well performance, future deliverabilities and recovery, and success of stimulation jobs.

During the current annual period, both a mathematical model describing gas flow through Devonian Shales and the software for a radial and one-dimensional mathematical model for the single well performance were completed and placed into operation. Experiments are being initiated in several related aspects of mass transfer in the tight matrix of Devonian Shales and the gas holding mechanism of the Devonian Shale matrix. Continued effort is underway in the development of a laboratory simulation model of Devonian Shales. Results from the laboratory experiment will be used to update the mathematical model developed. The sensitivity analysis of the mathematical model revealed some of the important parameters which greatly affect well performance. Field and laboratory measurement of these parameters will also be initiated.

Several radial and one-dimensional simulations of a Devonian Shale reservoir were performed to develop an understanding of the productivity of such reservoirs for a variety of different reservoir parameters. These simulation studies indicate the importance and range of reservoir parameters which are important in the either early or late production life of Devonian Shales.

The results of the simulation studies are as follows:

1. The sensitivity analysis showed that early performance of shale reservoirs is dominated by fracture system parameters, while later performance is primarily controlled by shale matrix and desorption parameters.
2. Gas slippage, or Klinkenberg effects, are pronounced in Devonian Shales, however, to date no experimental data are available for validation.
3. Fracture system permeability, shale matrix permeability and size, and desorption isotherms are determining factors of reservoir performance. However, data for these parameters is either scarce or non-existent.
4. By comparison, the dual-porosity desorption model had a 38 percent higher 30-year cumulative production than the Denver model.

2. RECOMMENDATIONS

As a result of the sensitivity study, reservoir performance appears to be strongly dependent on shale matrix parameters. This conclusion must be validated through laboratory experiments since a few assumptions were made about the transport and gas holding mechanism of the shale matrix. Battelle's laboratory experiments are expected to resolve this problem.

Permeability measurements on the shale matrix were limited to a small number of samples from a few wells. A new method should be designed to measure very low permeability of the shale matrix and Klinkenberg factors.

Fracture distributions should be related to shale permeability. A well test method should be designed to estimate fracture permeability. To date, well testing is the only method of determining a fracture system's permeability.

Because of the importance of well stimulation, it is suggested that efforts be continued to include stimulation boundary conditions into the present model.

The present radial, one-dimensional computer program should be extended into two to three dimensions to include the heterogeneity and anisotropy of shale reservoirs, and to make possible multiwell simulations. With a more complete and experimentally validated model, it would be possible to investigate some of the parameters which cannot be measured or determined directly using history matching technique.

3. INTRODUCTION

A recent trend in developing new natural gas reserves has been the intensified efforts to exploit Devonian Shale gas reservoirs in the Appalachian Basin. The Department of Energy (through the Morgantown Energy Technology Center, METC) is engaged in the Eastern Gas Shale Project, which is aimed at accelerating the economical development of this marginally productive resource.

Advances have been made in the modeling of Devonian Shale reservoirs in three main directions. The first direction is a general view of the many physical processes occurring in a Devonian Shale system. A general Devonian Shale reservoir model includes gas flow through fracture systems, flow into fracture systems from shale matrices, and desorption from pores of the shale matrix. It would be difficult to model such a general system in three dimensions. Attempts both theoretical as well as experimental, are being made to ascertain what needs to be studied. However, the experimental study is still in the planning stage.

The second direction is the formulation of a mathematical description of a much simplified system with an attempt to obtain an analytical solution. It has been possible to compare numerical with analytical results.

The third direction is research with a laboratory model to physically simulate gas transport through Devonian Shales. An attempt has been made to design an experimental procedure with the cooperation of Battelle.

Modeling efforts during the past year have been directed primarily at simulating isotropic homogeneous, radial, and one dimensional reservoir performance. It was felt that the need for a better understanding of the basic behavior of Devonian Shale performance was great enough to warrant this effort. Consideration has been given primarily to the study of desorption effects on reservoir performance. The flow model also considers Darcy's flow through the Devonian Shales including the Klinkenberg effect.

The results of the modeling effort have been used:

1. To determine the effect of reservoir parameters on reservoir performance.
2. To determine the possible range of the important parameters that will permit predicting of reserves and deliverability of production wells.
3. To improve the understanding of fracture and matrix systems in relation to the desorption process.

4. MATHEMATICAL MODEL

Most Devonian Shale reservoirs are expected to consist of very tight porous shale formations which may be rather highly fractured in certain tectonically and/or overburden stressed terranes. Under these conditions, the fractures may provide most of the gas permeability, but contribute very little to the overall storage capacity. By comparison, the matrix of the shale may provide most of the storage capacity, but contribute very little to flow because of the low permeability. The gas release and adsorption isotherm data from the Devonian Shale samples indicate that gas resides in the matrix of the shale as a free gas phase and as an adsorbed gas phase.¹ Figure 1 shows methane sorption isotherms at 28°C for the shale samples from the Illinois Basin.¹ In Figure 1, the upper curves measure the total gas content (free + adsorbed gas) as a function of pressure, while the lower curves measure physically adsorbed gas.

The transport of gas through any porous material is largely determined by the pore structure. Since the pore size of the shale matrix is small, gas slippage phenomena cannot be ignored. Moreover, gas desorbs from the pore walls into the shale matrix as pressure drops.

A fractured reservoir can be idealized^{2,3,4} as shown in Figure 2. All the fractures can be vertical (see model I in Figure 2), or all vertical and semi-vertical fractures can be replaced by an equivalent orthogonal fracture network (see model II in Figure 2). The mathematical formulation will be the same for both models. However, the approximation for the matrix block will be a cylindrical element for model I and a spherical element for model II.⁵

It is assumed that gas transport in Devonian Shale reservoirs occurs only in a porous fracture medium into which matrix blocks of contrasting physical properties deliver their gas contents. That is, the matrix acts as a uniformly distributed gas source in a fracture medium.⁴ Gas desorption from pore walls will be treated as a uniformly distributed source within the matrix blocks.

General assumptions made for the development of the mathematical model are as follows:

1. The reservoir has single phase gas flow.
2. The reservoir is horizontal with homogeneous matrix properties.
3. The reservoir is at an isothermal condition.
4. The well is centrally located in a finite circular reservoir.
5. Surface diffusion of adsorbed molecules on the walls of the pores will be neglected in the mathematical model. However, those gases which are adsorbed on pore walls pass through more efficiently than those which are not. For example, helium is not easily adsorbed at ordinary and higher temperatures and therefore, does not flow readily through a porous medium. The adsorbed phase must contribute to the overall flow. Thus, neglecting surface diffusion in the model will reduce the flow rate from the matrix.

The gas flow through the fracture systems can be described as:

$$\nabla \left[\frac{k_f}{\mu} \frac{p_f}{z} \nabla p_f \right] + \frac{p_f}{z} q_m = \frac{\partial}{\partial t} \left(\phi_f \frac{p_f}{z} \right) \quad (1)$$

Where:

k_f = fracture permeability, darcy

μ = viscosity, cp

ϕ_f = fracture porosity, dimensionless

p_f = fracture pressure, atm

t = time, sec

z = real gas deviation factor

q_m = volumetric flow rate per volume of shale matrix element,

$$\begin{aligned} & \text{cm}^3/\text{sec}/\text{cm}^3 \\ & = - \frac{A_m}{V_m} \frac{k_m}{\mu} \left(\frac{\partial p_m}{\partial n} \right) \text{ surface} \end{aligned}$$

A_m = surface area of matrix elements, cm^2

V_m = volume of matrix element, cm^3

n = normal direction to surface

The gas flow through the element of shale matrix, including the Klinkenberg effects, can be described as:

$$\nabla \left[\frac{k_x}{\mu} \frac{p_m}{z} \left(1 + \frac{b}{p_m} \right) \nabla p_m \right] = \phi_d \frac{\partial p_m}{\partial t} + \phi_m \frac{\partial}{\partial t} \left(\frac{p_m}{z} \right) \quad (2)$$

Where:

b = Klinkenberg factor

k_{gm} = permeability to gas, darcy

p_m = matrix pressure, atm

ϕ_m = matrix porosity

k_g = absolute permeability, darcy

\bar{p}_m = mean local pore pressure, atm

$\phi_d = \frac{dc_d}{dp} RT$, dimensionless

R = Universal gas constant, $\text{cm}^3 \cdot \text{atm} / \text{g mole K}$

T = Reservoir temperature, $^{\circ}\text{K}$

The source term in Eq. 1 can be determined from the solution of Eq. 2. The solution of Eq. 1 with respect to following initial and boundary conditions then gives the pressure distribution in a Devonian gas reservoir. Detailed development of the mathematical model is presented in Appendix A.

5. ANALYTICAL SOLUTIONS

The flow equations developed in previous sections for Devonian Shale gas are complex and not amenable to exact solution except under special conditions. Analytic solutions typically require very simple and idealized reservoir models and flow conditions (initial and boundary conditions and source/sink terms). Such results cannot be expected to model accurately all of the important features of real producing geophysical systems. Nonetheless, analytic solutions have received a considerable amount of attention, and they may contribute in several ways to the goal of predictive reservoir modeling.

At the most fundamental level, analytic solutions to idealized gas flow problems help to provide a better understanding of the basic flow phenomena. They may also be used to explore, in a very general and qualitative manner, the sensitivity of modeling predictions to a variety of different effects.

A much more immediate connection between analytic solution techniques and the modeling of real systems is the fact that many existing gas reservoir models actually involve a combination of both analytical and numerical methods. Typically, the detailed conceptual model of a real geologic system will contain elements which are thought to have a secondary, but significant effect on reservoir behavior. In order to keep the numerical analysis within manageable bounds, these elements might be approximated in a manner which allows an analytic solution. This solution is then combined interactively with numerical treatments of the other system elements within the overall numerical approach. Unfortunately, this type of approach may sometimes be motivated more by the need for a tractable model than by the reliability of the assumptions involved.

Because they do offer exact solutions to well-defined problems, analytic methods also provide very useful benchmarks for model testing and refining and for revealing potential problem areas with the more cumbersome (but hopefully much more powerful) numerical solution techniques. Certainly, the accuracy or reliability of any large-scale computer code should never be assumed without extensively testing the ability of that code to reproduce the results of a variety of exact analytic solutions. It must also be recognized that such comparisons still do not assure that the numerical routine will continue to be accurate and reliable when applied to more realistic and complex problems.

Another interesting and sometimes useful class of analytic solutions to flow equations arises in connection with the interpretation of well test flow data which are taken in order to learn about local in situ reservoir properties. Such well tests are extremely important as sources of the data needed to define reservoir model parameters. The analytic solutions used in well test analysis usually apply only to rather specialized (often very inconvenient) test conditions such as a well shut down after flowing at a constant rate (pressure buildup), or the opening of a shut-in well to a constant flow rate (pressure drawdown). The available analytic solutions also require highly idealized models of the reservoir properties near the well of interest. In practice, the required assumptions are never entirely fulfilled, and one is forced to choose between several qualitatively different "type curves," one of which must then be used to perform semi-quantitative interpretation of the data to obtain an estimate of local reservoir parameters. Despite the many difficulties, analytic solutions to well test problems have apparently been of significant value over the years in the petroleum industry. With the development of improved and more readily available numerical flow models, the use of analytic solutions

is now decreasing in favor of the more general-purpose computer methods. This is currently an active research and development area in the petroleum industry. Similar trends might be expected in connection with well test analyses.

In summary, much of the general, qualitative understanding of gas flow equations is based upon exact analytic solutions to special cases. In addition, these exact solutions are directly relevant to Devonian Shale gas reservoir modeling as a basis for testing and refining more powerful numerical solution methods. The importance of this role should not be underestimated, as the possibility of otherwise undetectable deficiencies in numerical calculations is very real. Although analytic solution methods have also been extensively employed (and still are to some extent) for special problems such as well test analysis, current emphasis is being placed on the development of more general-purpose numerical schemes. It should not be expected, however, that analytic solution methods alone will be capable of predictively modeling the detailed behavior of real Devonian Shale gas reservoirs.

The following simplifying assumptions in addition to the initial assumptions have been made in the development of the analytical solutions:

1. An isotropic finite reservoir of uniform thickness h .
2. All formation properties independent of pressure.
3. No Klinkenberg effect.
4. No desorption within the matrix elements.
5. Matrix elements consist of cylinders with radius \underline{a} and height h which are equal to the formation thickness.
6. Well produces at a constant pressure.

Under these conditions, Eq. 1 and initial and boundary conditions for the fracture system becomes:

$$\nabla \left[\frac{p_f}{z\mu} \nabla p_f \right] + \frac{p_f}{zk_f} q_m = \frac{\phi_f}{k_f} \frac{\partial}{\partial t} \left(\frac{p_f}{z} \right) \quad (3)$$

$$p_f(r,0) = p_i, \quad r_w \leq r \leq r_e \quad (3a)$$

$$p_f(r_w,t) = p_{wf}, \quad t > 0; \quad \text{constant flowing pressure at the wellbore} \quad (3b)$$

$$\left(\frac{\partial p_f}{\partial r} \right)_{r=r_e} = 0, \quad t > 0 \quad (3c)$$

Equation 2 and initial and boundary conditions for the matrix element become:

$$\left[\nabla \frac{p_m}{z\mu} \nabla p_m \right] = \frac{\phi_m}{k_m} \frac{\partial}{\partial t} \left(\frac{p_m}{z} \right) \quad (4)$$

$$p_m(r,0) = p_i, \quad 0 \leq r \leq a \quad (4a)$$

$$p_m(0,t) = \text{finite}, \quad t > 0 \quad (4b)$$

$$p_m(a,t) = p_f, \quad t > 0; \quad \text{at the surface of the matrix element} \quad (4c)$$

The solution of Eq. 3 in terms of pseudo-pressure with respect to initial and boundary conditions for a finite reservoir is developed in Appendix B and is given by:

$$\frac{\Delta\psi_f}{\Delta\psi_f} = \frac{\Delta\psi_{wf}}{s} \frac{U_0(\alpha, r_e, r)}{U_1(\alpha, r_w, r_e)} \quad (5)$$

Where:

ψ_f = fracture pseudo-pressure

s = Laplace space variable

$$\frac{1}{\eta(s)} = \frac{2k_m}{s\alpha k_f} \lambda \frac{I_1(\lambda a)}{I_0(\lambda a)} + \frac{1}{\eta_f}$$

$$\lambda^2 = s/\eta_m$$

I_1, I_0 = Modified Bessel function

$$\alpha^2 = \frac{s}{\eta(s)}$$

$$\Delta\psi_{wf} = \psi_i - \psi_{wf}$$

$$U_0(\alpha, r_e, r) = K_1(\alpha r_e) I_0(\alpha r) + I_1(\alpha r_e) K_0(\alpha r)$$

$$U_1(\alpha, r_w, r_e) = K_1(\alpha r_e) I_1(\alpha r_w) + I_1(\alpha r_e) K_0(\alpha r_w)$$

K_1, K_0 = Modified Bessel function

This equation gives the Laplace transform of the pseudo-pressure distribution in a finite-dual porosity gas reservoir producing at a constant pressure.

The volumetric flow rate entering the wellbore at a constant pressure is given as:

$$\bar{q}_{sc} = \frac{\gamma \Delta\psi_{wf}}{\sqrt{s} \eta(s)} \frac{U_2(\alpha, r_w, r_e)}{U_1(\alpha, r_w, r_e)} \quad (6)$$

Where:

$$\gamma = \pi k_f h r_w \frac{T_{sc}}{T_{p_{sc}}}$$

$$U_2(\alpha, r_w, r_e) = K_1(\alpha r_e) I_1(\alpha r_w) - I_1(\alpha r_e) K_1(\alpha r_w)$$

The exact inversion of Eq. 6 is complicated. Therefore, the flow rate (q_{sc}) is computed using a numerical Laplace transform inversion technique.

Further, the cumulative production (Q_{sc}) will be determined, which is related to q_{sc} , by:

$$Q_{sc} = \int_0^t q_{sc} dt' \quad (7)$$

The Laplace transform of Q_{sc} is:

$$\bar{Q}_{sc} = \frac{\bar{q}_{sc}}{s} = \frac{\gamma \Delta \psi_{wf}}{s^{3/2} \sqrt{\eta(s)}} \frac{U_2(\alpha, r_w, r_e)}{U_1(\alpha, r_w, r_e)} \quad (8)$$

This equation will also be inverted using the numerical Laplace transform inverter.

Computed values of Q_{sc} and q_{sc} from Eqs. 6 and 8 will be used to check the values of Q_{sc} and q_{sc} from the numerical solution.

6. NUMERICAL SOLUTIONS

Simultaneous solution of the equations presented above is achieved each time-step considering the following three principal aspects of the problem: (1) desorption of gas from pore walls of the shale matrix, (2) Darcy flow through the pores of the matrix into a fracture system considering the "Klinkenberg effect", and (3) Darcy flow through the fracture system to a producing well. Figure 3 shows the geometry of a one-dimensional radial model which will be used in simulating single well behavior with radial symmetry.

In the first stage, the production of gas from the wellbore causes a pressure drop in the fracture system. This in turn provides a reduced pressure on the outer surfaces of the shale matrix which causes Darcy flow modified by the Klinkenberg effect within the shale matrix. As this flow occurs, the pressure in the pores of the shale matrix decrease and gas is "fed" into the fracture system. Finally, this reduction in pressure within the pores of the shale matrix causes gas to be desorbed from the walls of the pores which provides "feed gas" to the matrix.

Once gas desorbs from the pore walls it flows through the shale matrix element to its outer surface where it can enter the fracture system via Darcy's law, giving the source term for the reservoir equation:

$$q_m = - \frac{A_m}{V_m} \frac{k_m}{\mu} \left(\frac{\partial p_m}{\partial r} \right)_{r=a} N_m$$

Here, a , A_m , and V_m are respectively, the radius, surface area, and volume of the matrix element and N_m is the number of elements per reservoir volume unit; i.e.:

$$N_m = \frac{\text{reservoir grid-block grain volume}}{\text{matrix element volume}}$$

For continuity of pressure at the matrix-fracture interface $(p_m)_{r=a}$ must equal p_f . Thus, the reservoir pressure serves as a boundary condition for the shale matrix element.

Using q_m as a source term for the radial diffusivity equation, together with a closed outer boundary and a specified rate or pressure at the wellbore, the reservoir pressure distribution as a function of time may be obtained. Details of the solution procedure are given in Appendix C. Care must be taken to assure that, at the end of each time-step, reservoir pressure, matrix element pressure, desorption rate, and source rate are consistent. The procedure described below was developed for this purpose.

Iterative Solution Procedure

Step 1. Begin new time-step by initializing matrix source rate q_m to zero and solving for reservoir pressure distribution, $p_f^{(m)}$; where m = number of iterations, $m = 1, 2, \dots$.

Step 2. Use reservoir pressure $p_f^{(m)}$, from Step 1 as a boundary condition to solve for matrix pressure $p_m^{(m)}$ and source rate q_m ; then use q_m to calculate new reservoir pressure, $p_f^{(m+1)}$.

Step 3. Set $m=m+1$ and calculate average of last two reservoir pressures, i.e.:

$$p_f^{(m)}(\text{avg}) = \frac{1}{2} \left(p_f^{(m)} + p_f^{(m-1)} \right)$$

Step 4. Use $p_f^{(m)}(\text{avg})$ as boundary condition to solve for new matrix pressure, $p_m^{(m+1)}$.

Step 5. Use $p_m^{(m+1)}$ and N_m to solve for new source rate q_m .

Step 6. Use new source rate to solve for new reservoir pressure, $p_f^{(m+1)}$.

Step 7. If $| p_f^{(m)} - p_f^{(m+1)} |$ is less than a specified tolerance, accept $p_f^{(m+1)}$ as the new reservoir pressure, and go to Step 1; otherwise, go to Step 3.

Wellbore conditions include the capability to simulate a variable rate or pressure history with skin damage and wellbore storage effects upon shut-in. A back pressure option is provided so that a specified wellhead pressure as a function of time may be used directly as input data.

The model consists of a main program, which has approximately 1000 lines of FORTRAN IV code, together with several subroutines for repetitive procedures such as transmissibility and bottom-hole pressure calculations. A user's manual including listing of the program is presented in Appendix D.

7. RESERVOIR-INPUT PARAMETERS

The Devonian Shale gas reservoir simulator requires input of all information describing the geometry of the flow system, shale and gas properties, adsorption and desorption properties of the shale matrix, the initial condition of the system, and wellbore conditions.

A simulation model may represent the behavior of laboratory equipment, individual wells, or reservoir systems. The simulator enables the engineer to examine and evaluate the physical and economic consequences of various alternative production policies. But a successful output from a simulator is really dependent on the reliability of the input data. Perhaps the most critical data are matrix and fracture permeabilities, Klinkenberg factors, fracture spacing and desorption data. Unfortunately, most of the necessary data for Devonian Shale reservoir simulations are not reliable. There are no available data for fracture spacing, geometry of the matrix elements, and desorption characteristics of the shale. In the following paragraphs, some of the data used in the simulator will be discussed.

Gas slippage, or Klinkenberg effects, are pronounced in Devonian Shales. Jones and Owens⁶ noted that the conventional extrapolative procedure (in which permeability plotted versus reciprocal arithmetic mean pressure is extrapolated to zero reciprocal pressure) for determining Klinkenberg permeability, k_{ℓ} , might not yield a straight line for very low permeability. Unfortunately, there are no experimental data to validate or refute this statement for the Devonian Shale.

The equation for the Klinkenberg "b" factor used in the simulator is given by:

$$b = 0.86 k_{\ell}^{-0.33} \quad (10)$$

Where:

$$b = \text{atm}$$

$$K_d = \text{md}$$

This equation is only valid for:

$$0.0001 \text{ md} < k_g < 1 \text{ md}$$

and the shale matrix permeability may go several orders of magnitude below 0.0001 md. Therefore, the "b" factor needs to be determined experimentally for shale samples. There is no systematic measurement of matrix permeability for Devonian Shales. Schettler⁷ et al. have presented some diffusion constant measurements at atmospheric pressure and an equation to relate permeability and the diffusion constant for the shale matrix.

Except for some measurements of high pressure adsorption isotherms for shale samples from the Illinois Basin¹ (as shown in Figure 1), and the work done by Schettler on shale samples, at atmospheric pressure, from Lincoln County, WV, there are practically no data available on the Devonian Shale.

As stated earlier, fracture spacing is an important parameter for which there is no known measurement technique. However, Muskat presented an equation for fracture permeability as:^{8,9}

$$k_f = \frac{10^8 W^3}{12 S} \text{ , darcy} \quad (11)$$

Where:

W = fracture width, cm.

S = fracture spacing, cm.

Figure 8 shows fracture spacing versus fracture permeability for various fracture openings as calculated from the above equation. Thus, if provided with good data on fracture permeability (determined from

reliable well test data) and fracture openings (measured from core samples), the fracture spacing can be approximated by Eq. 11.

The fracture permeability calculated from Eq. 11 usually yields high values because open tension fractures must be filled by an intruded foreign rock or a recrystallized component of the surrounding rock. In the Devonian Shale, fractures might be filled with either carbonate or pyritic material.^{10,11}

As a reservoir is produced, some permeability reduction in the fracture system might be expected because fractures created during stress conditions might become sealed after release of the stress.¹¹

As a last resort, the history matching technique with production or pressure data (or both) can be used to determine some of the reservoir parameters from the simulator. However, combinations of at least ten parameters for a typical Devonian Shale reservoir must be used to find a good match between field data and simulated data. Thus, the uniqueness of the matching may not be achieved if many permutations of the parameters are possible.

In summary, much of the general, qualitative and quantitative understanding of the gas transport mechanism and reservoir parameters have to be based on field and laboratory measurements. In order to make an engineering analysis, it is essential to determine and measure all of the necessary basic information about the actual Devonian Shale reservoir. Then a "sound" reservoir model can be build and simulation runs can be made. Otherwise, one may end up with a useless solution which is called "garbage in--garbage out!"

8. RESULTS OF SENSITIVITY ANALYSIS

Due to its complexity, the validity of the numerical model was impossible to prove for stability and convergence using current techniques of analysis. Therefore, it was necessary to conduct numerical experiments to evaluate the Devonian Shale reservoir simulation techniques described above. Use of finite difference approximations in the solution of Eqs. 1 and 2 introduce time and space truncation errors. If these truncation errors are sufficiently small, the numerical solution will be satisfactory. To evaluate the accuracy of these numerical solutions, the Devonian Shale gas simulator was used to calculate the performance of single and dual porosity models for which analytical solutions exist.

Slider¹² presented an equation for a single porosity gas reservoir producing at a constant pressure as:

$$Q_{MSCF} = \frac{0.111 \phi h r_w^2 c \left(p_i^2 - p_{wf}^2 \right) Q_{tD}}{z_{avg} T_f} \quad (12)$$

Q_{tD} can be read from the van Everdingen - Hurst¹³ table for a given t_D .

Where:

ϕ = porosity

h = formation thickness, ft.

r_w = wellbore radius, ft.

c = compressibility of gas, psia^{-1}

p_i = initial reservoir pressure, psia

p_{wf} = flowing wellbore pressure, psia

Q_{tD} = dimensionless cumulative production

z_{avg} = average compressibility factor, calculated at

$$(p_i + p_{wf}) / 2 \text{ and } T_f$$

T_f = formation temperature, R

$$t_D = \frac{6.33 \cdot 10^{-3} k t}{\phi \mu c r_w^2}$$

t = time, day

k = permeability, md

μ = viscosity, cp

Cumulative production values calculated from the simulator for a single porosity model should be the same as cumulative production calculated from Eq. 12. The differences in cumulative production values calculated from the simulator and Eq. 12 are less than two percent, even though Eq. 12 is not an exact solution of the unsteady-state gas flow.

By eliminating the desorption from the simulator, the model reduces to the dual porosity system described in the Analytical Methods section. The cumulative production results calculated from the analytical solution (Eq. 8) and from the simulator were presented in Figure 9. The numerical results were within two percent of the analytical solution. These comparisons show that the numerical solutions are of satisfactory accuracy for most engineering calculations.

The effects of reservoir parameters on the cumulative production of a Devonian Shale gas well which produces at two constant pressure flowing periods will be discussed. More specifically, the effects on production of fracture system parameters such as permeability and porosity, and shale matrix parameters such as permeability, porosity, Klinkenberg factor, desorption and size of the matrix element will be examined. For this series of parametric calculations, it is convenient to consider a base case and to vary parameters of interest around the value assumed in the base case. Parameters for the base case (roughly based on the Lincoln County, West Virginia DOE wells 20401, 20402, and 20403) are listed in Table 1.

Those parameters which are not known for these wells either are selected from other available data or are just assumed. Table 1 also presents possible ranges of the parameters which were used for the sensitivity analysis for a Devonian Shale gas reservoir. All the computations reported here were for a production period of 30 years.

The upper curve in Figure 10 represents cumulative production as a function of time for a dual-porosity model with desorption and Klinkenberg effects. The second curve from the top shows cumulative production as a function of time for a dual porosity model without desorption but includes Klinkenberg effects, while the third curve from the top does not include Klinkenberg effects. As noted previously, the gas slippage (Klinkenberg effect) factor is one of the important parameters which has considerable effects on gas production from Devonian Shales. The difference between the upper curve and second curve from the top is due to desorption from the pores of the shale matrix. These curves show that the effect of desorption is also important. The lower curve in Figure 10 represents cumulative production versus time for single porosity. It can be concluded that during the early life of the reservoir, the effects of matrix parameters with or without desorption on production are small. But after the initial flow period of a few years, gas from the matrix of the shale is very pronounced. The results of these calculations would seem to make a strong case for further investigation of the Klinkenberg and desorption effects on Devonian Shale gas production.

As discussed earlier in this paper, fracture system permeability, k_f , is one of the important parameters in Devonian Shale reservoirs as illustrated in Figure 11. This figure shows cumulative production as a function of time for various fracture permeabilities. All the reservoir parameters in these three cases are the same except k_f . The flow behavior of this model was dominated by the permeability of the fracture system.

Secondary porosity and desorption improve the well performance; in fact the well with a 933 feet drainage radius acts in an infinite system, even after 25-30 years of production. Long life of an individual well makes Devonian Shales a valuable resource even though production rate is usually low.

Figure 12 shows the shale matrix permeability, k_m , to be another important parameter which effects well productivity. As the matrix permeability decreases, the effect becomes very dominant. The dual porosity model behaves like a single porosity model if the matrix permeability is high enough (order of 10^{-7} md) and the size of the matrix element is small enough (order of 50 cm). In fact, the parameter k_m/a^2 (where: k_m = matrix permeability, a = radius of matrix element) can be treated as one of the major parameters controlling gas production from the shale matrix. The relationship between cumulative production and matrix permeability is not linear; i.e., if the permeability is increased from 0.69×10^{-9} md to 0.69×10^{-8} md the increment in cumulative production will be 8 percent. However if permeability is reduced from 0.69×10^{-9} md to 0.69×10^{-10} md the reduction in the cumulative production will be 18 percent in 30 years.

Figure 13 presents the cumulative production values for different fracture porosities (ϕ_f) as a function of time. The effects of fracture porosity on the cumulative production is almost negligible. The range of fracture porosity that is $\phi_f = 0.0025$ to 0.04 may be representative for Devonian Shales.

Figure 14 describes well performance for different values of matrix porosity (ϕ_m). Here the effect of matrix porosity on cumulative production is small. However, a maximum matrix porosity of 10 percent may be very low for Devonian Shales because the commercial mercury porosimeter has a lower limit of pore-diameter penetration of about 30^0 Angstrom¹ (\AA). But according to Ref. 1, the pore-diameters for Devonian Shales can be less than about 4^0 \AA .

Figure 15 shows that a twofold increase in matrix size causes about a 13 percent decrease in cumulative production. But a fivefold decrease in matrix size only causes a 7 percent increase in cumulative production. If the matrix permeability is greater than 10^{-7} this effect is almost negligible. But when matrix permeability decreases, the effect of matrix size will dominate well performance.

Figure 16 shows cumulative production for various drainage radii as a function of time. Here the effect of the outer boundary was felt by the well after about 6 years for $r_e = 500$ feet. However, cumulative production continues to increase as a function of time due to the contribution from the matrix element. A Devonian Shale reservoir with a drainage radius of 933 or 2000 feet acts as an infinite reservoir.

Figure 17 shows production rate versus time as a function of fracture system permeability (k_f). The rate decline is very slow as in the actual curves in Figure 6 of Ref. 14. Figure 17 also shows that the production decline is not an exponential decline as given in Ref. 15. The jump in the production rate after four years is due to a change in pressure at the wellhead. Figure 18 shows production rate as a function of time with and without the Klinkenberg effect. It can be seen from this figure that the Klinkenberg factor strongly affects the production history of Devonian Shale gas wells. Using the Klinkenberg factor in the model results in more than a one hundred percent increase in production rate.

Figure 19 shows a breakdown of resource recovery at low values of matrix permeability (k_m). Recovery factors are defined as follows:

$$r_t = \text{total recovery} = \frac{\text{total production}}{G_{iT}} = \frac{G_{iT} - G_r}{G_{iT}}$$

$$r_f = \text{recovery of initial gas in fracture system} = \frac{\text{gas produced from fractures}}{G_{if}} = \frac{G_{if} - G_f}{G_{if}}$$

$$r_m = \text{recovery of initial gas in matrix} = \frac{\text{gas produced from matrix}}{G_{im}} = \frac{G_{im} - G_m}{G_{im}}$$

$$r_d = \text{recovery of initial adsorbed gas} = \frac{\text{"desorbed" gas produced}}{G_{id}} = \frac{G_{id} - G_d}{G_{id}}$$

Where:

G_{if} = initial fracture gas

G_{im} = initial matrix gas

G_{id} = initial adsorbed gas

G_r = remaining total gas

G_f = remaining gas in the fracturing volume

G_m = remaining gas in the matrix

G_d = remaining gas adsorbed

$G_{iT} = G_{if} + G_{im} + G_{id}$

As matrix permeability approaches zero, a single porosity system is approached where gas is only produced from fracture systems. As k_m increases, the recovery of original fracture and matrix gas approaches a common value. For the base case value of k_m ($.69 \times 10^{-9}$), the matrix and fracture recovery was 26.2 percent at 30 years, which is close to the average of r_f and r_m in Figure 19. Note that as matrix permeability increases, the recovery of adsorbed gas increases since a higher k_m results in larger pressure drops in the shale matrix which in turn allows more gas to be desorbed. Of particular significance is the fact that for a low, but not unreasonable, matrix permeability of $.1 \times 10^{-10}$ md, the total resource recovery, r_t , is only 12 percent after 30 years.

Although the previous figures show the sensitivity of each parameter which affects the reservoir performance of Devonian Shales, a composite plot of all of the parameters is shown in Figure 20. In Figure 20 the abscissa denotes time and the ordinate denotes the percent increment or reduction in cumulative production. The percent change is defined as:

$$\text{percent change} = \left(\frac{Q_p - Q_B}{Q_B} \right) 100$$

Where:

Q_p = cumulative production for a given time and parameter

Q_B = cumulative production for the base case parameter

In previous paragraphs the effect of all of these parameters have been discussed. But the curves in this figure compare the effect of each parameter relative to other parameters. Again, fracture permeability, desorption, Klinkenberg slip factor, matrix size and permeability are the factors that determine Devonian Shale gas reservoir performance.

Figure 21 compares the cumulative production values using different mathematical models for Devonian Shales. As shown in this figure, the Denver model²⁴ (Cox's model) calculates the lowest values of cumulative production for the same set of reservoir parameters. Even the dual porosity model, without desorption and Klinkenberg effects, calculates a cumulative production of 16 percent more than the Denver model. The model including desorption and Klinkenberg effects calculates a cumulative production of 36 percent more than the Denver model at the end of 30 years.

NOMENCLATURE

| | |
|-----------------|---|
| a | Radius of shale matrix element, cm |
| c | Concentration, g mole/cm ³ |
| D | Diffusivity, cm ² /sec |
| k _f | Fracture permeability, Darcy |
| k _m | Matrix permeability, Darcy |
| M | Molecular weight, g-mole |
| q _m | Volumetric flow rate from matrix element, cm ³ /sec/cm ³ |
| q _{sc} | Production rate, cm ³ /sec |
| p _f | Fracture pressure, atm |
| p _i | Initial reservoir pressure, atm |
| p _m | Matrix pressure, atm |
| p _{wf} | Flowing well pressure, atm |
| r | Radius, cm |
| r _w | Well radius, cm |
| r _e | Drainage radius, cm |
| R | Universal gas constant, atm-cm ³ /g mole K |
| s | Laplace space time variable |
| T | Temperature, °K |
| w _m | Mass flow rate from shale matrix element, g/sec/cm ³ |
| t | Time, sec |
| z | Real gas deviation factor |
| φ _f | Fracture porosity |
| φ _m | Matrix porosity |
| ρ | Density of gas, g/cm ³ |
| ψ | Pseudo-pressure, atm ² /cp |
| μ | Viscosity of gas, cp |

REFERENCES

1. Thomas, J., Jr., and Frost, R. R.: "Internal Surface Area and Porosity in Eastern Gas Shales from the Sorption of Nitrogen, Carbon Dioxide, and Methane," in preprints of First Eastern Gas Shales Symposium, Morgantown, WV, Oct. 17-19, 1977.
2. Warren, J. E. and Root, P. J.: "The Behavior of Naturally Fractured Reservoirs," Soc. Pet. Eng. J. (Sept. 1963), p. 245-255.
3. Kazemi, H.: "Pressure Transient Analysis of Naturally Fractured Reservoirs with Uniform Fracture Distribution," Soc. Pet. Eng. J. (Dec. 1969), p. 451-462.
4. de Swaan, D. A.: "Analytical Solution for Determining Naturally Fractured Reservoir Properties by Well Testing," Soc. Pet. Eng. J. (June 1976), p. 112-117.
5. Ancell, K. L., Price, H. S., and Ford, W. K.: "An Investigation of the Gas Producing and Storage Mechanism of the Devonian Shale at Cottageville Field," SPE paper 2938, Presented at the SPE Symposium on Low Permeability Gas Reservoirs, SPE-AIME, Denver, CO, May 20-22, 1979.
6. Jones, F. O. and Owens, W. W.: "A Laboratory Study of Low Permeability Gas Sands," SPE paper 7551, Presented at the SPE Symposium on Low Permeability Gas Reservoirs, SPE-AIME, Denver, CO, May 20-22, 1979.
7. Schettler, P. D., Jr., Wampler, D. L., Sipling, P. J., and Mitchell, D. J.: "The Relationship of Thermodynamic and Kinetic Parameters to Well Production in Devonian Shale," in preprints of First Eastern Gas Shales Symposium, Morgantown, WV, Oct. 17-19, 1977, Morgantown Energy Research Center, p. 450-461.
8. Muskat, M.: The Flow of Homogeneous Fluids Through Porous Media, McGraw-Hill Book Co., Inc., New York (1937).
9. Elkins, F. L.: "Fractures in the Devonian Shale and the Spraberry," A letter to J. P. Brashear, Lewin and Associates, Inc., Sept. 8, 1979.
10. Kucuk, F., Alam, J., and Streib, D. L.: "Reservoir Engineering Aspects and Resource Assessment Methodology of Eastern Gas Shales," in preprints of Second Eastern Gas Shales Symposium, Morgantown, WV, Oct. 16-18, 1977.
11. De Sitter, L. W.: Structural Geology, McGraw-Hill Book Co., Inc., New York (1964), p. 70.
12. Slider, H. C.: Practical Petroleum Reservoir Engineering Methods, The Petroleum Publishing Co., Tulsa, OK (1976), p. 223-224.
13. van Everdingen, A. F., and Hurst, W.: "The Application of the Laplace Transformation to Flow Problems in Reservoirs," Trans., AIME, v. 186 (1949), p. 305-324.

14. Smith, E. C., Cremean, S. P., and Kozair, G.: "Gas Occurrence in the Devonian Shale," SPE paper 7921, presented at the SPE Symposium on Low Permeability Gas Reservoirs, SPE-AIME, Denver, C), May 20-22, 1979.
15. Kuuskraa, V. A., Brashear, J. P., Doscher, T. M., and Elkins, L. E.: "Enhanced Recovery of Unconventional Gas Sources," Section on Devonian Shale Gas of the Appalachian Basin, V. III (1978).
16. Klinkenberg, L. J.: "The Permeability of Porous Media to Liquids and Gases," Drilling and Production Practice (1941), p. 200-213.
17. Rose, W. D.: "Permeability and Gas-Slippage Phenomena," Trans., AIME (1948), v. 28, p. 127-135.
18. Al-Hussainy, R., Ramey, H. J., Jr., and Crawford, P. B.: "The Flow of Real Gases Through Porous Media," J. Pet. Tec. (May 1966), p. 624.
19. von Rosenberg, D. U.: Methods for the Numerical Solution of Partial Differential Equations, Elsevier Publishing Co., Inc., New York (1969).
20. van Poolen, H. C., Bixel, H. C., and Jargon, J. R., Reservoir Modeling, The Petroleum Publishing Co., Tulsa, OK.
21. Craft, B. C. and Hawkins, M. F.: Applied Petroleum Reservoir Engineering, Prentice-Hall, Inc., Englewood Cliffs, NJ (1959).
22. van Everdingen, A. F.: "The Skin Effect and Its Influence on the Productive Capacity of a Well," Trans., AIME (1953), v. 198, p. 171-176.
23. Katz, D. L., Cornell, D., Kobayashi, R., Poetmann, F. H., Vary, J. A., Elenbaas, J., and Weinaug, C. F.: Handbook of Natural Gas Engineering, McGraw-Hill Book Co., Inc., New York, NY (1959).
24. Science Applications, Inc., Denver, CO., "Engineering/Economic Evaluation of Eastern Gas Shale Enhanced Recovery Techniques", Briefing to Morgantown Energy Technology Center, Morgantown, August 1-2, 1979.

APPENDIX A

DEVELOPMENT OF FLOW MODEL FOR DEVONIAN SHALE RESERVOIRS

Under the assumption made in the main text, the gas flow through the fracture systems can be described by the following equation:

$$\nabla \left[\rho \frac{k_f}{\mu} \nabla p_f \right] + w_m(p_f, t) = \frac{\partial}{\partial t} (\phi_f \rho) \quad (A-1)$$

Where:

ρ = density, g/cm³

k_f = fracture permeability, darcy

μ = viscosity, cp

ϕ_f = fracture porosity

p_f = fracture pressure, atm

t = time, sec

w_m = mass flow rate per volume of shale matrix element,
g/sec/cm³

The equation of state for real gas is given by:

$$\rho = \frac{M}{RT} \frac{p_f}{z} \quad (A-2)$$

Where:

M = molecular weight, g mole

R = Universal gas constant, cm³ - atm/g mole K

T = Reservoir temperature, K

z = real gas deviation factor

Substitution of Eq. A-2 into Eq. A-1 yields Eq. 1 in the main text which is:

$$\nabla \left[\frac{k_f}{\mu} \frac{p_f}{z} \nabla p_f \right] + \frac{p_f}{z} q_m = \frac{\partial}{\partial t} \left(\phi_f \frac{p_f}{z} \right) \quad (A-3)$$

Where:

$$q_m = \text{volumetric flow rate per volume of shale matrix element,} \\ \text{cm}^3/\text{sec}/\text{cm}^3$$

$$= - \frac{A_m}{V_m} \frac{k_m}{\mu} \left(\frac{\partial p_m}{\partial n} \right) \text{ surface}$$

$$A_m = \text{surface area of matrix element, cm}^2$$

$$V_m = \text{volume of element, cm}^3$$

Equation A-3 describes gas flow through the fractured shale reservoir with a source term which is the contribution from the shale matrix. Gas transport through the matrix is also described by the diffusivity equation with a source term due to desorption of gas from the pore walls of the matrix. The following equation describes the motion of gas through the shale matrix.

$$\nabla \left[\rho_m \frac{k_{gm}}{\mu} \nabla p_m \right] + w_d = \frac{\partial}{\partial t} (\phi_m \rho_m) \quad (\text{A-4})$$

Where:

$$k_{gm} = \text{permeability to gas, darcy}$$

$$w_d = \text{desorption rate, g/sec/cm}^3 \text{ shale}$$

$$p_m = \text{matrix pressure, atm}$$

$$\phi_m = \text{matrix porosity}$$

The rate of desorption can be expressed as:

$$w_d = - M \left(\frac{dc_d}{dp_m} \right) \frac{\partial p_m}{\partial t} \quad (\text{A-5})$$

Where:

$$c_d = \text{concentration of gas at the surface of pore walls;} \\ \text{mole/cm}^3 \text{ shale}$$

$$\left(\frac{dc_d}{dp_m} \right) = \text{slope of gas desorption isotherm curve, mole/cm}^3 \text{ shale/atm}$$

The gas permeability of a porous medium usually exceeds the liquid permeability of the same medium. The difference in these permeabilities is due to the phenomenon known as gas slippage which is related to the mean free path of the gas molecules relative to pore diameter. Consequently, the gas permeability of a porous medium should be a function of the temperature, pressure, and the nature of the gas. Klinkenberg developed the relationship between gas permeability of a porous medium to a non-reactive liquid,^{16,17} viz:

$$k_g = k_\ell \left(1 + \frac{4C\bar{\lambda}}{r} \right) \quad (A-6)$$

This equation was derived assuming that all the capillaries in the porous medium are of the same diameter, and are oriented at random through the solid material. In Eq. A-6, k_g is gas permeability, k_ℓ is liquid permeability in a single phase completely filling the pores of the medium at constant temperature, $\bar{\lambda}$ is the mean free path of the gas molecules, r is the radius of capillaries, and C is a proportionality constant. The mean free path can be expressed as:

$$\bar{\lambda} = \frac{1}{\sqrt{2\pi} d^2 n} = \frac{RT}{\sqrt{2\pi} \bar{p}_m N d^2} \quad (A-7)$$

where d is collision diameter, n is concentration of molecules per unit volume, N is Avogadro's Number, \bar{p}_m is mean local pressure, T is temperature, and R is the universal gas constant. The following is obtained by combining Eqs. A-6 and A-7:

$$k_g = k_\ell \left(1 + \frac{4CRT}{\sqrt{2\pi} r N d^2 \bar{p}_m} \right) = k_\ell \left(1 + \frac{b}{\bar{p}_m} \right) \quad (A-8)$$

where b is the Klinkenberg factor, which is constant for a given gas and a given porous medium at a constant temperature. A graph of k_g vs. $1/\bar{p}_m$ should result in a straight line with an intercept of k_ℓ and a slope of $b k_\ell$.

Thus, gas permeability is greater at low pressures.

As can be seen from Eq. A-8, k_g is a function of mean pore pressure and pore diameter only because all other parameters are constant for a given gas and a given temperature. Since pore diameters are small for Devonian Shales, "b" is expected to be large. Therefore, the Klinkenberg effect or slippage factor cannot be ignored in the Devonian Shale model.

Substitution of Eqs. A-2, A-5, and A-8 into Eq. A-4 yields:

$$\nabla \left[\frac{k_{\ell}}{\mu} \frac{p_m}{z} \left(1 + \frac{b}{p_m} \right) \nabla p_m \right] = \phi_d \frac{\partial p_m}{\partial t} + \phi_m \frac{\partial}{\partial t} \left(\frac{p_m}{z} \right) \quad (A-9)$$

Where:

$$\phi_d = \left(\frac{dc_d}{dp} \right) RT, \text{ dimensionless}$$

The source term in Eq. A-3 can be determined from the solution of Eq. A-9. The solution of Eq. A-3 with respect to following initial and boundary conditions then gives the pressure distribution in a Devonian gas reservoir.

Initial Condition:

Initially the reservoir pressure will be assumed to be uniform and equal to p_i . Mathematically this can be stated as follows:

$$p(r,0) = p_i \quad (A-10)$$

Inner Boundary Condition:

For a general purpose simulation, the flow rate or pressure will be assumed to be a function of time at the inner boundary (wellbore). Mathematically, a variable rate or pressure condition can be expressed as:

$$\text{Variable rate: } \left(r \frac{\partial p(r,t)}{\partial r} \right)_{r=r_w} = \frac{q(t)\mu}{2\pi hk} \quad (A-11)$$

$$\text{Variable pressure: } p(r_w, t) = p_{wf}(t) \quad (A-12)$$

Outer Boundary Condition:

The reservoir will be assumed to be bounded with no flow at the outer boundary i.e."

$$\left(r \frac{\partial p(r,t)}{\partial r} \right)_{r=r_e} = 0$$

(A-13)

APPENDIX B
ANALYTICAL PROCEDURES

The flow in the fracture systems is given by Eq. 3, with respect to initial conditions Eq. 3a, and boundary conditions Eq. 3b and 3c. Equations 3 to 3c can be linearized by applying the pseudo-pressure transformation. The pseudo-pressure¹⁸, ψ , is defined as:

$$\psi_f = 2 \int_0^{p_f} \frac{p_f}{z\mu} dp_f \quad (B-1)$$

The variable ψ_f has the dimension of pressure-squared per centipoise. Equations 3 to 3c can be rewritten in terms of the pseudo-pressure in radial coordinates as:

$$\frac{1}{r} \frac{\partial}{\partial r} \left(r \frac{\partial \Delta\psi_f}{\partial r} \right) - \frac{2 k_m}{ak_f} \left(\frac{\partial \Delta\psi_m}{\partial r} \right)_{r=a} = \frac{1}{\eta_f} \frac{\partial \Delta\psi_f}{\partial t} \quad (B-2)$$

$$\Delta\psi_f (r,0) = 0 ; r_w \leq r \leq r_e \quad (B-3)$$

$$\Delta\psi_f (r_w,t) = \Delta\psi_{wf} ; t > 0 \quad (B-4)$$

$$\left(\frac{\partial \Delta\psi_f}{\partial r} \right)_{r=r_e} = 0 ; t > 0 \quad (B-5)$$

Where:

$$\Delta\psi_f = \psi_i - \psi_{wf}$$

$$\eta_f = \frac{k_f}{\phi_f \mu_i c_i}$$

To solve equation B-2, (subject to initial conditions Eq. B-3, and boundary conditions Eqs. B-4 and B-5) Eqs. B-1, B-4 and B-5 are transformed in Laplace space as:

$$\frac{1}{r} \frac{\partial}{\partial r} \left(r \frac{\partial \bar{\Delta}\psi_f}{r} \right) - \frac{k_m}{ak_f} \left(\frac{\partial \bar{\Delta}\psi_m}{r} \right)_{r=a} = \frac{s}{\eta_f} \bar{\Delta}\psi_f \quad (B-6)$$

$$\Delta\bar{\psi}_f(r) = \frac{1}{s} \Delta\bar{\psi}_{wf} \quad (B-7)$$

$$\left(\frac{\partial \bar{\Delta}\psi_f}{\partial r} \right)_{r=r_e} = 0 \quad (B-8)$$

To solve Eq. B-6, $\left(\frac{\partial \Delta\psi_m}{\partial r} \right)_{r=a}$ must be determined and therefore the flow equation for the matrix element must be solved.

The flow in the matrix element is given by Eq. 4, with initial and boundary conditions given by Eqs. 4a, 4b, and 4c. Equation 4 can be linearized by applying psuedo-pressure⁸ in radial coordinates as:

$$\frac{1}{r} \frac{\partial}{\partial r} \left(r \frac{\partial \Delta\psi_m}{\partial r} \right) = \frac{1}{\eta_m} \frac{\partial \Delta\psi_m}{\partial t} \quad (B-8)$$

Eq. B-8 will be solved for a cylindrical matrix element subject to the following initial and boundary conditions:

$$\Delta\psi_m(r,0) = 0 ; 0 \leq r \leq a \quad (B-9)$$

$$\Delta\psi_m(0,t) = \text{finite} ; t > 0 \quad (B-10)$$

$$\Delta\psi_m(a,t) = \Delta\psi_f, \text{ at the surface of the matrix element;} \quad (B-11)$$

$t > 0$

Where:

$$\Delta\psi_m = \psi_i - \psi_m$$

$$\eta_m = \frac{k_m}{\phi_m c_i \mu_i}$$

$$\psi_m = \int_0^{p_m} \frac{p_m}{z\mu} dp_m$$

The general solution of Eq. B-8 subject to Eqs. B-10 to B-11 in Laplace space is given by:

$$\Delta\bar{\psi}_m = \Delta\bar{\psi}_f I_0(\lambda r) / I_0(\lambda a) \quad (B-12)$$

Where:

$$\lambda^2 = \frac{s}{\eta_m}$$

Taking the derivative of Eq. B-12 with respect to r , and setting r equal to a yields:

$$\left(\frac{\partial \Delta \bar{\psi}_m}{\partial r} \right)_{r=a} = \lambda \Delta \bar{\psi}_f \frac{I_1(\lambda a)}{I_0(\lambda a)} \quad (\text{B-13})$$

Substitution of Eq. B-13 into Eq. B-6 yields:

$$\frac{1}{r} \frac{\partial}{\partial r} \left(r \frac{\partial \Delta \psi_f}{\partial r} \right) - \frac{s}{\eta(s)} \Delta \bar{\psi}_f = 0 \quad (\text{B-14})$$

Where:

$$\frac{1}{\eta(s)} = \frac{2 k_m}{s a k_f} \lambda \frac{I_1(\lambda a)}{I_0(\lambda a)} + \frac{1}{\eta_f}$$

The solution of this equation with respect to boundary conditions Eqs. B-7 and B-8 gives Eq. 5 shown in the main text.

APPENDIX C
NUMERICAL PROCEDURES

The flow equations for fracture systems and matrix elements are given by Eqs. 1 and 2 in the main text. These two equations must be coupled with the source term into the fracture system. The source term is given by:

$$q_m = - \frac{A_m}{V_m} \frac{k_m}{\mu} \left(\frac{\partial p_m}{\partial r} \right)_{r=a} N_m \quad (C-1)$$

Simultaneous solution of Eqs. 1 and 2 coupled with Eq. C-1 and the fact that p_f is a boundary condition for the matrix element, describes gas transport through the Devonian Shale.

In discussing finite-difference techniques for solving Eqs. 1 and 2, subscripts "f" and "m" will be dropped for simplicity and readability.

Solutions of Flow Equation for the Fracture System

Equation 1 may be efficiently solved numerically using the following stepwise procedure.

Step 1: Define a block-centered grid with radii defined as illustrated in Figure 4.

Step 2: Write the finite-difference approximation of Eq. 1 for node i over a time interval Δt as:

$$\frac{T_{sc}}{p_{sc} T} \left[\frac{1}{r_i} \left(\frac{pk}{\mu z} \frac{\partial p}{\partial \ln r} \right)_{i+\frac{1}{2}} - \left(\frac{pk}{\mu z} \frac{\partial p}{\partial \ln r} \right)_{i-\frac{1}{2}} \right] + (q_{sc})_i = \quad (C-2)$$

$$(r_{i+1} - r_i)$$

$$\frac{T_{sc} \phi_i}{p_{sc} T \Delta t} \left[(p/z)_i^{n+1} - (p/z)_i^n \right]$$

Superscript "n" denotes time and q_{sc} is the source rate in SCF/day/cu.ft.

Step 3: Expanding the flow terms in Eq. C-2 at the grid block boundaries, using the relationship for radial flow through beds in series, and multiplying Eq. C-2 by the grid block volume the implicit-difference form becomes:

$$TR_{i-\frac{1}{2}}^{n+1} (p_{i-1}^{n+1} - p_i^{n+1}) + TR_{i+\frac{1}{2}}^{n+1} (p_{i+1}^{n+1} - p_i^{n+1}) + \quad (C-3)$$

$$(q_{sc})_i = r_i \left[(p/z)_i^{n+1} - (p/z)_i^n \right]$$

Where:

$$TR_{i-\frac{1}{2}}^{n+1} = \pi h \left(\frac{T_{sc}}{p_{sc} T} \right) TM_{i-\frac{1}{2}} (p_{i-1}^{n+1} + p_i^{n+1})$$

= interblock transmissibility

$$r_i = \frac{T_{sc}}{p_{sc} T} \frac{(V_p)_i}{\Delta t}$$

V_p = pore volume

$$TM_{i-\frac{1}{2}} = \frac{k_{i-1} k_i}{k_i (\mu z)_{i-1} \ln(r_i/\bar{r}_{i-1}) + k_{i-1} (\mu z)_i \ln(\bar{r}_i/r_i)} .$$

$(q_{sc})_i$ = SCF/day

The grid block volume used in Eq. C-2 is defined as:

$$V_i = 2\pi k \bar{r}_i (r_{i+1} - r_i) \quad (C-4)$$

Step 4: Expand the p/z term on the RHS of Eq. C-2 to get:

$$(p/z)_i^{n+1} - (p/z)_i^n = p_i^n \left(\frac{1}{z_i^{n+1}} - \frac{1}{z_i^n} \right) + \frac{1}{z_i^{n+1}} (p_i^{n+1} - p_i^n) \quad (C-5)$$

Step 5: Define an iteration scheme for solving Eq. C-3 with the RHS expanded as in Eq. C-5. Begin with old time level values for $TR_{i-\frac{1}{2}}$ and z_i^{n+1} in Eq. C-5; then iterate until no further change in pressure is observed; i.e., if "*" denotes the latest calculated values for p and z then Eq. C-2 can be written as:

$$TR_{i-\frac{1}{2}}^* \left(p_{i-1}^{n+1} - p_i^{n+1} \right) + TR_{i+\frac{1}{2}}^* \left(p_{i+1}^{n+1} - p_i^{n+1} \right) + (q_{sc})_i = \quad (C-6)$$

$$r_i \left[p_i^n \left(\frac{1}{z_i^*} - \frac{1}{z_i^n} \right) + \frac{1}{z_i^*} \left(p_i^{n+1} - p_i^n \right) \right]$$

Equation C-6 can be written as a tri-diagonal system:

$$a_i p_{i-1}^{n+1} + b_i p_i^{n+1} + c_i p_{i+1}^{n+1} = d_i \quad (C-7)$$

Where:

$$a_i = TR_{i-\frac{1}{2}}^*$$

$$b_i = TR_{i-\frac{1}{2}}^* - TR_{i+\frac{1}{2}}^* - r_i/z_i^*$$

$$c_i = TR_{i+\frac{1}{2}}^*$$

$$d_i = -(q_{sc})_i - r_i \left(p_i^n / z_i^n \right)$$

The Thomas Algorithm¹⁹ may be used to solve the system of equations given in Eq. C-7 for new reservoir pressures. TR^* 's and z^* 's are then recalculated and the process is repeated until the maximum change in pressure at any node is less than some specified tolerance. Note that at convergence, z_i^* will be essentially equal to z_i^{n+1} .

This iterative procedure is described by van Poolen²⁰ and has been found to work very well. Usually it will converge in two or three iterations and seldom requires more than six iterations, even for very large changes in wellbore conditions.

Boundary Conditions: The external reservoir radius is closed which is easily accomplished in the Thomas Algorithm by setting:

$$c_N = TR_{N+\frac{1}{2}} = 0 \quad (C-8)$$

where N is the outermost node.

The internal reservoir radius will be less than the wellbore radius and will also be closed by setting:

$$a_1 = TR_{1+\frac{1}{2}} = 0. \quad (C-9)$$

Thus, node 1 will actually be "within the wellbore" as shown in Figure 5. This permits easily specifying either a constant rate or a constant pressure over any time-step.

Solution of the Flow Equation for the Matrix Element

Solution of Eq. 2 may be accomplished using the same basic procedure described above. Subscript "j" will be used to distinguish the matrix equations from the reservoir finite-difference equations.

The Klinkenberg term can be handled by using the relationship:

$$(k_m)_j = k_L (1 + b/p_j^n) \quad (C-10)$$

An additional term due to the desorption in the matrix flow equation is present. The finite difference-scheme for Eq. 2 is as follows:

$$TR_{j-\frac{1}{2}}^{n+1} \begin{pmatrix} p_{j-1}^{n+1} & - p_j^{n+1} \end{pmatrix} + TR_{j+\frac{1}{2}}^{n+1} \begin{pmatrix} p_{j+1}^{n+1} & - p_j^{n+1} \end{pmatrix} = \quad (C-11)$$

$$\Gamma_j p_j^n \left[\left(\frac{1}{z_j^*} - \frac{1}{z_j^n} \right) + \frac{1}{z_j^*} \left(p_j^{n+1} - p_j^n \right) \right] +$$

$$\frac{V_j}{\Delta t} \left(\frac{dc}{dp} \right) p_j^{**} \left(p_j^{n+1} - p_j^n \right)$$

where: ** denotes the average of p_j^* and p_j^n .

A tri-diagonal system is again present as:

$$a_j p_{j-1}^{n+1} + b_j p_j^{n+1} + c_j p_{j+1}^{n+1} = d_j \quad (C-12)$$

where:

$$= a_j = TR_{j-\frac{1}{2}}^*$$

$$b_j = - TR_{j-\frac{1}{2}}^* - TR_{j+\frac{1}{2}}^* - \frac{\Gamma_j}{z_j^*} - \frac{V_j}{\Delta t} \left(\frac{dc}{dp} \right) p_j^{**}$$

$$= c_j = TR_{j+\frac{1}{2}}^*$$

$$d_j = - \left[\frac{j}{z_j} + \frac{V_j}{\Delta t} \left(\frac{dc}{dp} \right) p_j^{**} \right] p_j^n$$

The Thomas Algorithm and the iterative procedure described in the previous section may again be used to solve Eq. C-12.

Boundary Conditions for the Matrix Element

The pressure in the outermost node will be held constant (over a time-step) at the prevailing fracture pressure of the reservoir node in which the matrix element lies as in Figure 6.

Source Term for Reservoir Equation

In order to evaluate the source terms $(q_{sc})_i$ in Eq. C-3 we observe that the flow rate out of the matrix elements within reservoir block i due to holding p_j constant at $p_{f,i}$ is:

$$(q_{sc})_i = TR_{j-\frac{1}{2}} (p_{m,j-1} - p_{f,i}) (N_m)_i \quad (C-13)$$

Where: $p_{f,i}$ and $p_{m,j}$ denote the fracture and the matrix pressure respectively, $TR_{j-\frac{1}{2}}$ = transmissibility between the two outer matrix nodes:

$$(N_m)_i = \frac{(r_{i+1}^2 - r_i^2)(1 - \phi_i)}{a^2} \quad (C-14)$$

In developing the code it was found that the use of Eq. C-13 sometimes gave inconsistent results with $a = 10$ cm due to the very small distances and very small pressure drops involved. Thus, an alternative method is used which determines q_{sc} from material balance considerations as shown below:

$$(q_{sc})_i = \left\{ \left[\begin{array}{l} \text{decrease in gas} \\ \text{content over} \\ \text{time-step} \end{array} \right]_i + \left[\begin{array}{l} \text{amount of gas} \\ \text{desorbed over} \\ \text{time-step} \end{array} \right] \right\} \frac{1}{\Delta t} \quad (C-15)$$

It was determined by comparison with both analytical and numerical models that the pressure distribution within the matrix element was correct.

APPENDIX D

USER PROCEDURE AND PROGRAM LISTING

1. WELLBORE OPTIONS

In addition to the capability to specify any rate or pressure each time-step, the numerical model has the following options and special features:

1.1 Skin damage. As presented by Craft and Hawkins,²¹ the "infinitesimal" skin factor, s , introduced by van Everdingen²² can be related to a finite damaged zone of radius r_{skin} and permeability k_d as follows:

$$s = \frac{k - k_d}{k_d} \ln \left(\frac{r_{skin}}{r_w} \right) \quad (D-1)$$

In the finite-difference model it is convenient to take $r_3 = r_{skin}$ as shown in Figure 7. Thus, for any specified skin factor, we can solve Eq. (D-1) for the correct value of k_d to find:

$$k_d = \frac{k_2}{1 + \frac{s}{\ln(r_3/r_w)}} \quad (D-2)$$

Where k_2 is the undamaged permeability of Node 2.

1.2 Wellbore storage (afterflow). If the wellbore (tubing and annulus) is full of fluid at the time of shut-in, which is nearly always the case for gas wells, the sand-face rate after shut-in must satisfy

$$q_{sc} B_g dt = V_w c_w dp \quad (D-3)$$

Solving for q_{sc} and using the definition of gas formation volume factor gives

$$q_{sc} = \frac{T_{sc} \dot{p}}{p_{sc} T z} V_w c_w \frac{dp}{dt} \quad (D-4)$$

For a real gas, the compressibility of the wellbore fluid, c_w , becomes

$$c_g = \frac{1}{p} - \frac{1}{z} \frac{dz}{dp} \quad (D-5)$$

This gives, after some manipulation,

$$q_{sc} = \frac{T_{sc} V_w}{p_{sc} T} \frac{d(p/z)}{dt} \quad (D-6)$$

In finite-difference form Eq. D-6 is

$$q_{sc}^{n+1/2} = \frac{T_{sc} V_w}{p_{sc} T} \frac{1}{\Delta t} \left[(p/z)^{n+1} - (p/z)^n \right] \quad (D-7)$$

Equation D-7 is used for the wellbore storage in the numerical simulator.

Since node 1 is 'within the wellbore' in the reservoir grid system, it is only necessary to assign the entire wellbore volume to this node in order to simulate wellbore storage effects after the well is shut-in. Of course, the calculated node 1 pressure will then be the average wellbore pressure.

1.3 Back pressure equation. The Cullender-Smith Equation²³ solved for bottom-hole pressure is:

$$p_{bh}^2 = e^S p_{wh}^2 + \frac{q_{MCFD}^2 G T_a z_a f X}{40000 d^5} \left(\frac{e^S - 1}{S} \right) \quad (D-8)$$

Where:

G = gas gravity

T_a = average wellbore temperature, deg R

z_a = average gas deviation factor

f = friction factor

X = well depth, ft.

d = tubing ID, in.

p_{wh} = wellhead pressure, psia

p_{bh} = bottom-hole pressure, psia

$$S = .0375 G X/T_a z_a.$$

The friction factor is given as a function of Reynolds Number(RE) and pipe roughness in Figure 7-3 of Katz²³.

For laminar flow($600 < RE < 2100$) f is given by

$$f = 64/RE \quad (D-9)$$

If RE is greater than 4000, f may be obtained by solving

$$1/f^{1/2} = 2 \log(d/e) + 1.14 - 2 \log\left[1 + 9.34 (d/e)/RE f^{1/2}\right] \quad (D-10)$$

where e is absolute pipe roughness in inches. The Reynolds Number is given by

$$RE = 20 q_{MCFD} G/\mu d \quad (D-11)$$

A subroutine FRIC has been written to solve Eq. D-10 for f using the Newton-Raphson technique. The routine also uses Eq. D-9 for laminar flow, sets f to zero for RE less than 600, and uses a default value (specified by the user) for the critical range ($2100 < RE < 4000$).

Another subroutine (PBH) uses the value of f determined by FRIC in Eq. D-8 to calculate bottom hole pressure, p_{bh} , given values of wellhead pressure and other parameters. Since z_a depends upon the average pressure, and p_{bh} is not a priori known, an iterative procedure is required. Once p_{bh} is calculated z_a is updated and the calculations repeated until p_{bh} stabilizes.

Also, since q depends on p_{bh} in the simulator, iteration must be performed at the end of each time-step using

$$q_{av} = 0.5 (q^n + q^{n+1}) \quad (D-12)$$

Of course, each time a new rate is used the friction factor must be updated. The point is that at the end of each time-step the values of bottom-hole pressure, production rate, friction rate, and z-factor are consistent.

These options provide a very powerful tool for studying gas well performance. In fact, together with the capability to vary rate or pressure as a function of time, virtually any gas well test or production performance can be simulated, with or without the effects of the dual porosity system and gas desorption.

2. DATA PREPARATION

The code is written in FORTRAN IV with some IBM extensions. Unless otherwise specified, integer and real variables are read with I5 and F10.0 format specifications, respectively. The simulation model consists of a calling program with several subroutines for performing special functions such as the calculation of interblock transmissibilities and bottom-hole pressures.

All data are read by the main program in this model. Detailed instructions for preparing input data are given below. Where the designation 'title card' appears, the card may contain any desired information.

Input Data

1. Title Card
2. Reservoir & Wellhead Temperature & Shale Density --- FORMAT(3F10.0)
T
TSURF
RHOSH
3. Title Card
4. Gas Gravity & Wellbore Parameters ----- FORMAT(7F10.0)
GR ----- Gas specific gravity
DIA ----- Tubing ID (in)
E ----- Tubing roughness (in)
X ----- Well depth (ft)
DFTV ----- Default value for friction factor
ODIA ----- Tubing OD (in)
CSGID ----- Casing ID (in)

5. Title Card
6. Number of Gas Property Cards to be Read ---- FORMAT(I5)
NT1
7. Gas Property Table ----- FORMAT(3F10.0)
PT1 ----- Pressure (psia)
VIS ----- Viscosity (cp)
ZT ----- z-factor
NT1 cards are read.
8. Title Card
9. Number of Values in Isotherm Table ----- FORMAT(I5)
NT0
10. Isotherm Table ----- FORMAT(2F10.0)
PT ----- Pressure (psia)
CT ----- Concentration(cc @ STP/gm)
NT0 cards will be read.
11. Title Card
12. Initial Parameters for Isotherm Equation --- FORMAT(2F10.0)
B1
B2
See comments in program listing for details. Note that if B1=0.0,
no desorption will occur giving a 'dual porosity' simulator.
13. Title Card

14. Reservoir Grid Parameters ----- FORMAT(I5,2F10.0)
NR ----- Number of grid-blocks
ALPHA ----- Geometric multiplier
DR(1) ----- Size of first grid-block
I ----- Grid-block index
DR(I) ----- Size of grid-block I (ft)
See comments in program listing for details. Note that since a
block-centered grid is used, the outer radius will have index NR+1.

15. Title Card

16. Reservoir Thickness ----- FORMAT(F10.0)

H

17. Title Card

18. Reservoir Grid Data ----- FORMAT(I5,3F10.0)

I ----- Grid-block index

PHI(I) ----- Porosity

K(I) ----- Permeability(md)

P(I) ----- Initial pressure (psia)

19. Title Card

20. Skin Factor ----- FORMAT(F10.0)

S

If S=0.0, nothing happens; if S is positive, the node 2 permeability
is altered as explained in the section on Wellbore Options; negative
values of S are not permitted.

21. Title Card

22. Klinkenberg Parameters ----- FORMAT(3F10.0)
 BK ----- Klinkenberg factor 'b'
 C1 ----- Parameters for Klinkenberg
 C2 ----- equation
 If BK=0.0, b=0; if BK is positive, b=BK; if BK is negative, b is
 determined from $b = C1 k_1^{-C2}$, where k_1 is the absolute matrix permeability.
23. Title Card
24. Matrix Element Parameters ----- FORMAT(15,F10.0)
 NRM ----- Number of matrix element grid-blocks
 ARAD ----- Matrix element radius(cm)
25. Title Card
26. Normalized Cumulative Radii ----- FORMAT(15,F10.0)
 J ----- Matrix element grid-block index
 RAN(J) ----- Cumulative radii
 Note that, since a block-centered grid is used, the outer radius will
 have index NRM+1.
27. Title Card
28. Matrix Element Properties ----- FORMAT(F10.0,E11,4)
 PHIM ----- Porosity
 KLM ----- Permeability(md)
29. Title Card
30. Master Code ----- FORMAT(15)
 MCODE

If MCODE = 0, all matrix element calculations are bypassed giving a standard 'single porosity' radial gas simulator. If MCODE = 1, a normal run will occur; if MCODE = 2 a normal run will also occur, but with suppression of any matrix element grid-block pressures greater than the initial pressure. This was found to be necessary in one or two cases involving low reservoir porosities to avoid physically unreal adsorption rates due to intermediate calculated pressures (i.e. before convergence) one or two psi higher than the original pressure.

31. Title Card

32. Title Card

33. Variable Pressure Parameters ----- FORMAT(2I5)

NVPN ----- Number of different pressures

KBACK ----- Back pressure 'switch'

If KBACK = 0, all specified pressures are assumed to be bottom-hole flowing pressures. If KBACK = 1, all specified pressures are used as flowing wellhead pressures and the bottom-hole pressure is calculated as explained in the section on Wellbore Options.

34. Well Pressure History ----- FORMAT(F7.0,4x,4F8.0,5x,
4F8.0)

PWL ----- Well pressure(psia)

D1 ----- Day
H1 ----- Hour
M1 ----- Minute
SEC1 ----- Second

"on time"
for PWL

D2 ----- Day
H2 ----- Hour
M2 ----- Minute
SEC2 ----- Second

"off time"
for PWL

The value of PWL is assigned as the well pressure whenever "on time" < simulation time (@ end of step) \leq "off time". Note that NVPN cards are read.

35. Title Card

36. Title Card

37. Number of Variable Rates ----- FORMAT(I5)

NVQN

38. Well Rate History ----- FORMAT(F7.0,4x,4F8.0,5x,
rF8.0)

QV ----- Well production rate (MCFD)

| | | |
|-------------------|---|-----------|
| D1 ----- Day | } | "on time" |
| H1 ----- Hour | | |
| M1 ----- Minute | | |
| SEC1 ----- Second | | |

for
rate QV

| | | |
|-------------------|---|------------|
| D2 ----- Day | } | "off time" |
| H2 ----- Hour | | |
| M2 ----- Minute | | |
| SEC2 ----- Second | | |

for
rate QV

The value of QV is assigned as the well production rate whenever "on time" < simulation time (@ end of step) \leq "off time". Note that NVQN cards are read.

39. Title Card

40. Wellbore Storage Parameter ----- FORMAT(I5)

KSTOR

The parameter KSTOR has no effect unless the well is shut-in. Upon shut-in, a non-zero value of KSTOR causes the node 1 volume to be altered to include the actual wellbore volume (tubing & annulus) so that afterflow may occur. For details see the Wellbore Options section.

41. Title Card

42. Run Parameters ----- FORMAT(I5,5F10.0,I5)

NMAX ----- Maximum number of time-steps

TMAX ----- Maximum simulation time

ERR ----- Reservoir pressure cycle tolerance

ERRM ----- Matrix pressure cycle tolerance

ERRF ----- Tolerance for iteration procedure

DPW ----- Tolerance for bottom-hole pressure calcs.

KT1 ----- Skip print parameter

A complete printout will be obtained every KT1th time-step, including the first and last step. The convergence pressure tolerances should be in the range 0.1 to 0.001. ERRF has the most effect on reservoir material balance errors.

43. Title Card

44. Time-step Sizes ----- FORMAT(4F10.0)

DAY

HOUR

MIN

SEC

As many cards as desired may be read. For each card read, the time-step size is converted to days for internal use. If N cards are read, all time-steps after step N will be the same as step N.

3. COMPUTER PROGRAM LISTING

```

//WKSUNGAS JOB (CS2803F4,3017)
/*JOBPARM I=8,L=9
/*ROUTE PRINT RMT1)
// EXEC FC@TGCLG,PARM.FORT='NCSOURCE',PARM.LKED='LET,LIST',REGION=200K
//FORT.SYSIN DD *
IMPLICIT REAL*8 (A-F,O-Z)

C
C***** ----- UNGAS -----
C
C      RADIAL FLOW MODEL FOR (UNCONVENTIONAL) GAS PRODUCTION FROM DEVONIAN SHALE
C      DEVELOPED FOR SCIENCE APPLICATIONS, INC., MORGANTOWN, WV
C
C***** ARRAYS FOR (FRACTURED) RESERVOIR
REAL*8 K(40),K1(40),MCFI,MCFC,MCFA,IMBE,MEE,NSC
DIMENSION DR(41),TR(41),VP(40),TP1(50),TP2(50),PWL(50),TQ1(50),
ETQ2(50),GV(50),PHI(40),OSC(40),P(40),PN(40),PG(40),PF(40),
EPSTAR(40),BG(40),VIS(40),Z(40),ZN(40),GAMMA(40),BKLF(40)
E,QW(50),PW(50),PWH(50),CUMPRD(50),CUMINJ(50),FCZAVG(50),
EFT(500),QM(500),QD(500),CUMDSP(500),CUMP(40),CUMI(40)
C
C***** ARRAYS FOR MATRIX ELEMENT
REAL*8 KLM,KGM(20),MCFMI,MCFDI,MCFMA,IMBEM(40),MBEM(40),
ENE(40),INJN,MCFDA,INJ(40),NSC#(40),MBEMM
DIMENSION RAN(21),RA(21),VCLM(20),VPM(20),FM(40,20),FMN(40,20),
EPMG(20),PMSTAR(20),VISM(20),ZM(40,20),ZMN(40,20),
ETRM(21),GAMJ(20),AZM(20),BZM(20),CZM(20),DZM(20)
E,QQ(40),A(2,2),FF(2,50),BB(2),GSCC(40),GASM1(40),GMCAL(40),GMN(40)
E,GACT(40),PRD(40),POLD(40)
C
C***** ARRAYS FOR GENERAL USE
INTEGER*2 HEADIN(40),PFLAG,CFLAG,SFLAG,IR(40)
REAL*8 M1,M2,MIN
DIMENSION FT(50),CT(50),YE(50),DEV(50),AZ(40),EZ(40),CZ(40),
E0Z(40),EZ(41),FZ(41),UZ(40),PT1(50),ZT(50),DUM(50),DLM1(50)
C
C
C      DATA PSC,TSC,IND,ETI/14.7,529.,0.0,0.0/
C      DATA TR,TRM,GAMJ,CUMPRD,PWH/A1*0.0,21*0.0,20*0.0,500*0.0,500*(0.0/
C      DATA CUMINJ,CUMDSP,QM,QD,GMCAL/500*0.0,500*0.0,500*0.0,500*0.0,
C      S40*0.0/CUMP,CUMI/40*0.0,40*0.0/
C      DATA MBE,RVCL,MCFI,MCFC,MCF#/0.0,0.0,0.0,0.0,0.0/
C
C      DATA RVCLM,MCFMI,MCFDI,MCFMA/0.0,0.0,0.0,0.0/
C      DATA NRMAX,NRMMAX/40,20/
C
C      FC(X,B1,52)=E1*X/(1.+B2*X)
C      DFDX(X,Y,Z)=Y/((1.+Z*X)*(1.+Z*X))
C
C      FK(X,A,B) = A*X**B
C
C
C      AZ(1)=0.0
C      NRMM=NRMAX+1
C      NRMAT=NRMMAX+1
C
C***** READ RESERVOIR & WELLHEAD TEMPERATURE & SHALE DENSITY
READ 69,HEADIN
READ 137,T,TSURF,RHCSH
PRINT 91,T,TSURF,RHOSH
T=T+460.
TSURF=TSURF+460.
TA=0.5*(T+TSURF)
CCN=PSC*T*1000./TSC
CON1=1./CON
C
C
C      READ 69,HEADIN
C      READ 137,GR,DIA,E,X,DFTV,DDIA,CSG10
C      PRINT 177,GR,DIA,E,X,DFTV,DDIA,CSG10
C      A1=GR*TA*X/(4000)*DIA**5)
C      A2=.0375*GR*X/TA
C
C
C***** READ GAS VISCOSITY & Z-FACTORS DATA
READ 69,HEADIN
READ 1,NT1
READ 9,(PT1(L),VIS(L),ZT(L),L=1,NT1)
PRINT 93
PRINT 95
PRINT 97,(PT1(L),VIS(L),ZT(L),L=1,NT1)
C
C***** READ ISOTHERM TABLE
READ 69,HEADIN
READ 1,NT0

```

```

READ 201,(PT(J),CT(J),J=1,NTQ)
PRINT 99
PRINT 101
PRINT 103,(PT(J),CT(J),J=1,NTQ)
C**** NOW CONVERT TO DESIRED UNITS (PSIA & SCF/CU FT)
C CONSTANT 1.0569 CONVERTS FROM 0 DEG C TO 60 DEG F
C (NOTE THAT CC AT SC/CU CM = SCF/CU FT)
C DO 200 J=1,NTQ
C PT(J)=PT(J)*14.7
200 CT(J)=CT(J)*RHCSH*1.0569
C**** DETERMINE LEAST SQUARES COEFFICIENTS
C READ INITIAL ESTIMATES OF COEFFICIENTS B1 & B2 IN THE EQUATION
C  $C = B1 * P / (1 + B2 * P)$ 
C NOTE: USUALLY THE LAST DATA POINT WORKS WELL AS AN INITIAL GUESS
C HOWEVER, IF B1 IS READ AS ZERO, NO DESCRIPTION WILL OCCUR
C
READ 69, HEADIN
READ 137,B1,B2
BB(1)=B1
BB(2)=B2
IK=2
IF(B1.LE.1.E-4) PRINT 1370
IF(B1.GT.1.E-6)
CALL NLLSQS(IK,NTQ,PT,CT,A,BB,CZ,FF,EZ,YE,DEV,OLM,DUM1)
B1=BB(1)
B2=BB(2)
C
C**** ESTABLISH RESERVOIR GRID DIMENSIONS
C
READ 69,HEADIN
READ 1,NR,ALPHA,DR(1)
NR1=NR+1
PRINT 3,NR
IF(DR(1).LE.0.0) GO TO 104
IF DR(1).LE.ZERO READ ALL DR(I)'S
IF(DR(1).GT.ZERO USE ALPHA TO CALCULATE OTHERS
DO 102 I=2,NR1
102 DR(I)=ALPHA*DR(I-1)
GO TO 110
104 READ 51,(1,DR(I),I=1,NR1)
C CALCULATE GRID-BLOCK CENTERS
110 DO 106 I=2,NR1
106 DUM(I-1)=0.5*(DR(I-1)+DR(I))
C
PRINT 5
PRINT 7,(1,DR(I),DUM(I),I=1,NR)
PRINT 7,NR1,DR(NR1)
C
C**** READ RESERVOIR GRID DATA (ARRAY PF1 AVAILABLE AFTER VP IS CALC.)
READ 69,HEADIN
READ 137,H
PRINT 11,H
VWELL= 3.14159*0.25 * (CSGID*CSGID - (CDIA*CDIA-DIA*DIA)) * X/144.
TPI = 3.14159 * .006328 * CON1 * H
PRINT 181,A1,A2,VWELL,TPI
READ 69,HEADIN
READ 13,(1,PHI(I),K(I),P(I),I=1,NR)
PRINT 15
PRINT 17,(1,PHI(I),K(I),P(I),I=1,NR)
C PHI IS FRACTURE POROSITY (NATURAL FRACTURES)
C K IS FRACTURE PERMEABILITY
C P IS INITIAL PRESSURE IN FRACTURE SYSTEM
C PM IS INITIAL PRESSURE IN SHALE MATRIX
C
DO 214 I=1,NR
PF(I)=P(I)
IR(I)=I
214 PN(I)=P(I)
C
C**** READ SKIN FACTOR (MUST BE POSITIVE)
READ 69,HEADIN
READ 137,S
IF(S.LE.1.E-5) GO TO 216
K(2)=K(2)/(1. + S/DLOG(DR(3)*DR(2)))
PRINT 175,S,K(2)
C
C**** READ KLINKENBERG FACTOR
216 READ 69,HEADIN
READ 137,BK,C1,C2
IF(BK.LT.0.0) PRINT 3109,C1,C2
IF(EK.GE.0.0) PRINT 3111,BK
C
C**** ESTABLISH MATRIX ELEMENT GRID DIMENSIONS
READ 69,HEADIN

```

```

      READ 51,NRM,ARAD
      NRM1=NRM+1
      PRINT 19,ARAD
C**** READ NORMALIZED CUMULATIVE RAQII
      READ 69,HEADIN
      READ 51,(J,RAN(J),J=1,NRM1)
      DO 120 J=1,NRM1
120    RA(J)=RAN(J)*ARAD
      PRINT 21
      PRINT 23,(J,RAN(J),RA(J),J=1,NRM1)
C**** VC CONVERT RA TO FEET
      DO 125 J=1,NRM1
125    RA(J)=RA(J)/30.48
      ARAD=ARAD/30.48
      ARAD2=ARAD*ARAD
-
C**** READ MATRIX GRID DATA(PHIM & KLM)
      READ 69,HEADIN
      HY=H
      READ 1377,PHIM,KLM
      PRINT 1777,PHIM,KLM
-
C**** READ MATRIX CODE (IF MCODE=0 ALL MATRIX CALCULATIONS WILL BE BYPASSED)
      READ 69,HEADIN
      READ 1,MCODE
      IF(MCODE.EQ.0) PRINT 3115
C
      IF(MCODE.EQ.0) GO TO 258
C**** INITIALIZE MATRIX PRESSURES & Z-FACTORS
      DO 218 I=1,NR
      PP=P(I)
      CALL INTFP1(PT1,ZT,NT1,PP,ZZ)
      DO 218 J=1,NRM
      ZA(I,J)=ZZ
      PM(I,J)=P(I)
218    CONTINUE
C
C**** CALCULATE NUMBER OF MATRIX ELEMENTS IN EACH GRID-BLOCK
      NE(1)=0.0
      DO 256 I=2,NR
      NE(I)=(DR(I+1)*CR(I+1) - DR(I)*DR(I)) * (1.-PHI(I))/ARAD2
256    CONTINUE
C
C
C**** CALCULATE PORE VOLUME & INITIAL GAS IN PLACE
C ----- FRACTURES -----
258    PRINT 115
      PRINT 109
      DO 250 I=1,NR
      VOL=3.14159*(DR(I+1)*DR(I+1)-DR(I)*DR(I))*H
      VP(I)=PHI(I)*VOL
      RVOL=RVOL+VP(I)
      PP=P(I)
      CALL INTRP1(PT1,ZT,NT1,PP,ZZ)
      BG(I)=CCN*ZZ/PP
      GAS=VP(I)/BG(I)
      MCFI=MCFI+GAS
      Z(I)=ZZ
      IF(MCODE.EQ.0) GO TO 248
      GMD = .001*(1.-PHI(I)) * VOL * B1 * F(I)/(1. + E2*P(I))
      VCFDI = MCFDI + GMD
248    PRINT 111,I,VOL,VP(I),RVOL,ZZ,BG(I),GAS,VCFI,MCFDI
250    CONTINUE
      DRVOL=1./RVOL
C
      IF(MCODE.EQ.0) GO TO 268
C ----- MATRIX -----
C (ASSUME INITIAL MATRIX PRESSURE = LOCAL FRACTURE PRESSURE)
      PRINT 117
      PRINT 113
      DO 260 J=1,NRM
      VOLM(J)=3.14159*(RA(J+1)*RA(J+1)-RA(J)*RA(J))*HY
      VPM(J)=PHIM*VOLM(J)
      RVCLM=RVCLM+VPM(J)
      PRINT 111,J,VOLM(J),VPM(J),RVCLM
260    CONTINUE
C
      PRINT 205
      DO 265 I=1,NR
      PP=P(I)
      CALL INTRP1(PT1,ZT,NT1,PP,ZZ)
      BGM=CCN*ZZ/PP
      GASM=RVCLM/BGM
      GASM1(I)=GASM*NE(I)

```

```

MCFMI=MCFMI+GASMI(I)
PRINT 111,I,BGMM,GASM,NE(I),GASMI(I),MCFMI
266 CCONTINUE
C**** ESTABLISH WELL PRESSURE HISTCFY
C---- BOTTOMHOLE PRESSURES- IF KEACK = 0
C---- WELLHEAD PRESSURES IF KEACK = 1
C
268 READ 69,HEADIN
READ 69,HEADIN
READ 183,NVFN,KEACK
IF(KBACK.EQ.1) PRINT 193
KP=KBACK
IF(NVFN.EQ.0) GO TO 272
IF(KP.EQ.0)PRINT 129
IF(KP.EQ.1)PRINT 185
PRINT 131
DO 270 L=1,NVFN
READ 125,PWL(L),D1,H1,M1,SEC1,C2,F2,M2,SEC2
PRINT 127,PWL(L),D1,H1,M1,SEC1,D2,H2,M2,SEC2
TP1(L) = D1 + H1/24. + M1/1440. + SEC1/86400.
TP2(L) = D2 + H2/24. + M2/1440. + SEC2/86400.
270 CONTINUE
272 CONTINUE
C
C**** ESTABLISH WELL PRODUCTION HISTCFY
C
READ 69,HEADIN
READ 69,HEADIN
READ 1,NVGN
IF(NVGN.EQ.0) GO TO 282
PRINT 167
PRINT 169
DO 280 L=1,NVGN
READ 125,CV(L),D1,H1,M1,SEC1,C2,F2,M2,SEC2
PRINT 127,CV(L),D1,H1,M1,SEC1,D2,H2,M2,SEC2
TQ1(L) = D1 + H1/24. + M1/1440. + SEC1/86400.
TQ2(L) = D2 + H2/24. + M2/1440. + SEC2/86400.
280 CONTINUE
282 CONTINUE
C
C**** READ WELLBORE STORAGE PARAMETER
READ 69,HEADIN
READ 1,KSTOR
IF(KSTOR.NE.0) PRINT 191
KS=KSTOR
C
C**** READ RUN PARAMETERS
READ 69,HEADIN
READ 133,NMAX,TMAX,ERR,ERRM,ERRF,DPW,KT1
PRINT 135,NMAX,TMAX,ERR,ERRM,ERRF,DPW,KT1
KT=KT1
C
C**** PRINT INITIAL INVENTORY OF GAS IN PLACE
PRINT 3123
PRINT 3117
PRINT 3119,MCFI,MCFMI,MCFDI
TGAS = MCFI + MCFMI + MCFDI
FGF = MCFI/TGAS * 100.
FGM = MCFMI/TGAS * 100.
FGD = MCFDI/TGAS * 100.
PRINT 3121,TGAS,FGF,FGM,FGD
PRINT 3123
C
C
C**** ENTER TIME-STEP LCCP
C
READ 69,HEADIN
IF(BK.LT.0.0) BKL=FK(KLM,C1,C2)
IF(BK.LT.0.0) PRINT 4709, KLM,C1,C2,EKL
4709 FORMAT(/T15,'PARAMETERS KLM,C1,C2,EKL ARE: ',4E15.6//)
C
IF(BK.GE.0.0) EKL = BK
C
DO 284 I=1,NF
K1(I)=K(I)
XKF=K(I)
IF(BK.LT.0.0) BKLF(I)=FK(XKF,C1,C2)
IF(BK.LT.0.0) PRINT 4711,K(I),K1(I),XKF,C1,C2,EKLF(I)
IF(BK.GE.0.0) EKLF(I)=EK
284 CONTINUE
4711 FORMAT(/T2,'VALUES OF K(I),K1(I),XKF,C1,C2,BKLF(I) ARE: ',6E11.4//)
C

```

```

NR 41=NRM-1
DO 100) N=1,NMAX
QW(N)=0.0
SFLAG=0
QFLAG=0
KCY=0
DP=1000.
DPPW=1000.
KNT=0
IF(N.GT.1)ETI=ETI+DELT
IF(IND.EQ.0) READ (5,137,END=2000) DAY,HOUR,MIN,SEC
IF(IND.EQ.0) DELT = DAY + HOUR/24. + MIN/1440. + SEC/86400.
511 FT(N)=ETI+DELT
IF(N.EQ.1 .OR. N.EQ.NMAX .OR. N.LEO.KT)
PRINT 333,N,ETI,DELT
DIV=1./DELT
IF(ETI+.5*DELT.GE.TMAX)GO TO 1001
C
C**** INITIALIZE SOURCE TERMS, STORE 'N-LEVEL' VALUES, & CALC GAMMA & GAMJ
DO 290 I=1,NR
GSC(I)=0.0
GSCC(I)=0.0
PM(I)=P(I)
ZN(I)=Z(I)
GAMMA(I)=CCN1*VF(I)*DIV
290 CONTINUE
C
IF(VCODE.EG.0) GO TO 560
C
DO 292 I=1,NR
DO 292 J=1,NRM
PM(I,J)=PM(I,J)
ZM(I,J)=ZM(I,J)
292 CONTINUE
C
DO 300 J=1,NRM
GAMJ(J)=CCN1*VM(J)*DIV
300 CONTINUE
C
KCYPF=0
540) KCYPF=KCYPF+1
IF(KCYPF.GT.99) PRINT 4707,DP
IF(KCYPF.GT.99)STOP
IF(KCYPF.EG.1) GO TO 560
C
C**** STORE FRACTURE PRESSURES & RATES(DSC) FROM LAST CYCLE
DO 5410 I=1,NR
Q(I)=GSC(I)
IF(I.GT.1)GSC(I)=0.0
POLD(I)=PF(I)
P(I)=0.5*(PF(I)+P(I))
IF(KCYPF.GT.10) P(I)=0.5*(P(I)+POLD(I))
5410 PF(I)=P(I)
C
C**** RESET MATRIX PRESSURES
DO 5420 I=1,NR
DO 5420 J=1,NRM
5420 PM(I,J)=PMN(I,J)
C
C**** CALCULATE NEW MATRIX PRESSURES & GAS INFLUX IN EACH RESERVOIR GRID-BLOCK
C
DO 3100 I=2,NR
AZM(NRM)=0.0
BZM(NRM)=1.0
CZM(NRM)=0.0
DZM(NRM)=P(I)
KCYM=0
C
5600 KCYM=KCYM+1
C
FIRST CALCULATE "KLINKENBERG" PERMEABILITIES
DO 2998 J=1,NRM
KG(J)=KLM*(1. + EKLM/PM(I,J))
2998 CONTINUE
C
NOW CALCULATE MATRIX TRANSMISSIBILITIES(TRM)
DO 3006 J=1,NRM
PP=PV(I,J)
CALL INTRP1(PT1,ZT,NT1,PP,ZZ)
CALL INTRP1(PT1,VIS,NT1,PP,VS)
ZM(I,J)=ZZ
DUM(J)=VS
VIS(J)=VS
DUM(J)=PP
3006 CONTINUE
C

```

```

C      IF(N.EQ.1.AND.KCYM.LE.2)PRINT 207
C
C      CALL TRND(NRM,DUM,TRM,KGM,RA,DUM1,VISM,TP1)
C      IF(N.GT.1.OR.KCYM.GT.2)GO TO 3103
C      DO 3102 J=1,NRM
C      PRINT 145,ZM(I,J),VISM(J),DUM(J),TAM(J),EKL,KGM(J),PM(I,J)
C      CONTINUE
C**** DETERMINE ISOTHERM SLOPE FOR EACH MATRIX ELEMENT NODE
C
3103 CONTINUE
C      IF(N.EQ.1.AND.KCYM.LE.2)PRINT 3103
C      DO 3111 J=1,NRM
C      PFM=J.5*(FM(I,J)+FMN(I,J))
C      DUM(J) = DFDX(PFM,B1,B2)
C      DUM1(J) = .001*VCLM(J)*DIV*DUM(J)
C      IF(N.GT.1.OR.KCYM.GT.2)GO TO 3010
C      PRINT 3107,J,GAMJ(J),DUM(J),DUM1(J)
3010 CONTINUE
C
C**** SET UP TRIDIAGONAL MATRIX USING PRESERVE NODE PRESSURE AS BOUNDARY COND.
C
C      DO 3012 J=1,NFM1
C      AZM(J)=TRM(J)
C      CZM(J)=TRM(J+1)
C      BZM(J)=-AZM(J)-CZM(J)-GAMJ(J)/ZM(I,J) + DUM1(J)
3012 DZM(J) = - (GAMJ(J)/ZMN(I,J) + DUM1(J) + FMN(I,J))
C
C**** STORE LATEST PRESSURES & SOLVE FOR NEW MATRIX ELEMENT PRESSURES AT NODE I
C      DO 3014 J=1,NRM
3014 PHI(J)=PM(I,J)
C      CALL LTRI(NFM,AZM,EZM,CZM,DZM,EZ,FZ,UZ)
C
C      IF(N.EQ.1.AND.KCYM.LE.2)PRINT 1411
C      IF(N.GT.1.OR.KCYM.GT.2)GO TO 3020
C      DO 3016 J=1,NRM
C      PRINT 111,J,AZM(J),BZM(J),CZM(J),DZM(J),PHI(J),UZ(J)
C      CONTINUE
3016 CONTINUE
3020 CONTINUE
C
C**** CHECK FOR CONVERGENCE
C      DP=DABS(UZ(1)-PHI(1))
C      DO 3030 J=2,NFM
C      DPM=DABS(UZ(J)-PHI(J))
C      IF(DPM.GT.DP)DP=DPM
3030 CONTINUE
C
C      DO 3042 J=1,NRM
3042 PM(I,J)=UZ(J)
C
C      IF(KCYM.GT.99.OR.UZ(NRM).LT.0)STOP
C      IF((N.EQ.1.OR.N.EC.NMAX.OR.N.EC.KT).AND.DP.LT.ERRM)
C      PRINT 1611,KCYM,I,DP,UZ(NRM)
C      IF(DP.LT.ERRM)GO TO 3044
C      GO TO 5600
C
3044 CONTINUE
C
C      IF(E1.LE.1.E-6)GO TO 3056
C      QDD=J.0
C      DO 3054 J=1,NRM
C      IF(MCODE.EC.2.AND.PM(I,J).GT,PMN(I,J))PM(I,J) = PMN(I,J)
C      PPM=PM(I,J)
C      PPMN=PMN(I,J)
C      QDD = QDD + VCLM(J)*(FC(PFM,E1,B2) - FC(PFM,E1,B2))
3054 CONTINUE
C      QSCD(I) = .001*DIV*QDD*NE(I)
3056 CONTINUE
C
C      IF(KCYPF.EC.2)GMN(I)=GMCAL(I)
C      IF(N.EQ.1)GMN(I)=GASM1(I)
C      GSM=J.0
C
C      DO 4606 J=1,NRM
C      PPM=PM(I,J)
C      CALL INTRP1(PT1,ZT,NT1,PPM,ZZ#)
C      BGM=CGN+ZZM/PPM
C      GSM=GSM+VPM(J)/EGP
4606 CONTINUE
C
C      GMCAL(I) = GSM*NE(I)
C      INJ(I)=QSCD(I)*DELT
C      PRD(I)=GMN(I) -GMCAL(I) +INJ(I)

```

```

OSC(I)=PRD(I)*DIV
IF(KCYPF.GT.5) QSC(I) = 0.5*(QSC(I)+GO(I))
IF(KCYPF.GT.15) QSC(I) = 0.5*(QSC(I)+GO(I))
C IF(N.EQ.1.OR.N.EQ.NMAX.OR.N.EQ.KT) PRINT E113,I
C IF(N.EQ.1.OR.N.EQ.NMAX.OR.N.EQ.KT)
EPRINT 3103,(PM(I,J),J=1,NRM),QSC(I),QSCD(I)
310) CONTINUE
C
560 KCY =KCY+1
C
C**** CALCULATE INTER-BLOCK TRANSMISSIBILITIES(TF)
C
DO 31) I=1,NR
PP=P(I)
CALL INTRP1(PT1,ZT,NT1,PP,ZZ)
CALL INTRP1(PT1,VIS,NT1,PP,VS)
Z(I)=ZZ
VIS(I)=VS
K(I)= K1(I) * (1. + 3KLF(I)/PP)
310) CONTINUE
C
C IF(N.EQ.1)PRINT 139
CALL TRND(NR,P,TR,K,DR,Z,VIS,TF1)
C IF(N.GT.1)GO TO 326
C DO 320 I=1,NR
C PRINT 111,I,DR(I),VIS(I),Z(I),K(I),TR(I),GAMMA(I)
C2) CONTINUE
326 CONTINUE
C
C**** ESTABLISH WELL PFEASURE OR PRODUCTION RATE THIS TIME-STEP
C
C**** NOTE THAT ARRAY PW IS ALWAYS USED TO STORE NODE 1. PRESSURE;
C HENCE IS NORMALLY BOTTOM-HOLE PRESSURE (BUT IS AVG WELLEDRE
C PRESSURE IF WELLBORE STORAGE OPTICA IS IN EFFECT)
C
IF(KCY.GT.1)GO TO 3988
KNT=KNT+1
IF(N.GT.1.AND.KNT.GT.1)GO TO 355E
PFLAG=0
IF(NVPN.EQ.?) GO TO 394
C
C
DO 39) L=1,NVPN
IF(PFLAG.NE.0) GO TO 3988
IF(FT(N).LE.TP1(L).OR.FT(N).GT.TP2(L)) GO TO 390
PFLAG=L
QZ(1)=1.0
CZ(1)=0.0
C
IF(KP.EQ.0) GO TO 386
C**** USE CULLENDER-SMITH EQUATION TO CALCULATE EFP
C
IF(N.EQ.1 .AND. KNT.EQ.1) IFY=1
IF(N.EQ.1 .AND. KNT.GT.1) IFY=2
IF(N.GT.1 .AND. KNT.EQ.1) IFY=3
C
IF(IFY.EQ.1) QAV=0.0
IF(IFY.EQ.1) PBH1=PWL(L)
C
IF(IFY.EQ.2) QAV=QW(1)
IF(IFY.EQ.2) PBH1=BHP
C
IF(IFY.EQ.3) QAV=QW(N-1)
IF(IFY.EQ.3) PBH1=PW(N-1)
C
VS=VIS(1)
CALL FRIC(QAV,GR,VS,DIA,E,RE,F,IF,DFTV)
PWH(N)=PWL(PFLAG)
PHEAD=PWH(N)
CALL PBH(A1,A2,QAV,F,PBH1,PHEAD,DPW,PT1,ZT,NT1,PBF2,ZAV,PAV,IEHP)
C PRINT 189,QAV,RE,F,IF,PBH2,IEHP
C
BHP=PBH2
OZ(1)=BHP
C
GO TO 390
C
386 OZ(1)=PWL(L)
PRINT 143,PWL(L)
C
390 CONTINUE

```

```

394 IF(NVGN.EQ.0) GO TO 398
DC 396 L=1,NVGN
IF(FT(N).LE.TG1(L).CR.FT(N).GT.TG2(L))GO TC 356
OFLAG=L
OSC(1)=-OV(L)
PRINT 171,OV(L)
C
395 CCONTINUE
C
398 CONTINUE
C
C**** IF WELL IS SHUT-IN SEE IF WELLCORE STORAGE OPTION HAS BEEN SELECTED
C
IF(PFLAG.EQ.0) .AND. OFLAG.EQ.0) .AND. KS.NE.0) SFLAG=1
IF(SFLAG.EQ.0) GO TO 3988
GAMMA(1) = VWELL*COM1*DIV
PRINT 195
C
C
C
C**** SET UP TRIDIAGONAL MATRIX
3988 DO 350 I=1,NR
IF(I.EQ.1) .AND. PFLAG.NE.0) GO TO 350
AZ(I)=TR(I)
CZ(I)=TR(I+1)
BZ(I) = - AZ(I) - CZ(I) - GAMMA(I)/Z(I)
DZ(I) = - OSC(I) - GAMMA(I)*PN(I)/ZN(I)
350 CONTINUE
C
C
C**** STORE LATEST PRESSURES & SOLVE FOR NEW (RESERVOIR) PRESSURES
C
DO 400 I=1,NR
400 PG(I)=P(I)
C
CALL LTRI(NR,AZ,BZ,CZ,DZ,EZ,FZ,P)
C
IF(N.EQ.1)PRINT 141
IF(N.GT.1)GO TC 416
DC 410 I=1,NR
PRINT 111,I,AZ(I),BZ(I),CZ(I),DZ(I),PG(I),F(I)
410 CONTINUE
416 CONTINUE
C
C**** CHECK FOR CONVERGENCE
DP = DABS(P(1) - PG(1))
DO 440 I=2,NR
DM=DABS(P(I) - PG(I))
IF(DM.GT.DP)DP=DM
440 CONTINUE
C
IF(P(1).LT.0.0) PRINT 203
IF(P(1).LT.0.0) STOP
IF(KCY.GT.99) PRINT 199
IF(KCY.GT.99) STOP
C
IF((N.EQ.1.OR.N.EQ.NMAX.OR.N.EQ.KT) .AND. LP.LT.ERR)
C
PRINT 161,KCY,N,DP,P(1),P(2)
IF(DP .LT. ERR) GO TO 460
C
GO TO 560
C
C
460 KCY=1
C
C**** CALCULATE (OR STORE) PRODUCTION RATE & WELL PRESSURE THIS STEP
C
IF(PFLAG.NE.0) .CR. SFLAG.NE.0) QW(N) = TR(2) + (F(2) - P(1))
IF(SFLAG.NE.0) GO TO 4604
IF(OFLAG.NE.0) QW(N) = -OSC(1)
IF(OFLAG.NE.0) .CR. PFLAG.EQ.0) .CR. KP.EQ.0) GO TO 4604
IF(N.GT.1)GO TO 4598
IF(PFLAG.NE.0) .AND. KP.EQ.1) .AND. KNT.EQ.1) GO TO 560
C
MUST GO BACK AND DO BHP CALCULATION WITH QW(1)
C
QAV=QW(1)
GO TO 4600
C
4598 QAV=0.5*(QW(N-1) + QW(N))
4600 BPH=BHP
C
VS=VIS(1)
CALL FRIC(QAV,GR,VS,DIA,E,PE,F,IF,DFTV)
PWH(N)=PWL(PFLAG)

```

```

PHEAD=PWH(N)
CALL PBH(A1,A2,QAV,F,PBH1,PHEAD,DPW,PT1,ZT,NT1,P3H2,ZAV,PAV,IEHP)
C
C
PRINT 189,QAV,RE,F,IF,PBH2,IEHP
C
DPPW=PBH2-EHP
C
PRINT 197,KCY,KNT,SHP,P3H2,DRFW
IF(DABS(DPPW).LT.DPW) GO TO 4602
SHP=PBH2
P(1)=SHP
DZ(1)=SHP
C
GO TO 56)
C
4602 IF((N.EQ.1,CR.N.EG.NMAX,CR.N.EG.KT) .AND. (KF.EG.1))
PRINT 187,PWH(N),P(1)
C
4604 CONTINUE
C
IF(MCODE.EQ.0) GO TO 4620
C
IF(KCYPF.EQ.1) GO TO 5400
C
C**** NOW MUST CHECK ON CONVERGENCE OF FRACTURE PRESSURES
DP=DABS(P(1) - PF(1))
DO 4610 I=1,NR
DM=DABS(P(I) - PF(I))
IF(DM.GT.DP)DP=DM
4610 CONTINUE
C
IF((N.EQ.1,DR.N.EG.KT,CR.N.EG.NMAX) .AND. (DF.LT.ERRF))
PRINT 1661, KCYPF,N,DP,P(1),P(2)
IF(DP.LT.ERRF) GO TO 4620
C
GO TO 5400)
C
4620 IF(SFLAG.NE.0) GAMMA(1)=V2(1)*CLN1*DIV
PW(N)=P(1)
PRCDN=QW(N)*DELT
INJN=0.0
DSP=0.0
IF(MCODE.EQ.0) GO TO 4632
DO 4630 I=2,NR
DSP=DSP+INJ(I)
INJN=INJN+PRD(I)
4630 CONTINUE
C
4632 IF(N.EQ.1)CUMPRD(1)=PRCDN
IF(N.EQ.1)CUMINJ(1)=INJN
IF(N.EQ.1)CUMDSP(1)=DSP
IF(N.EQ.1)GO TO 430
CUMPRD(N) = CUMPRD(N-1) + PRCDN
CUMINJ(N) = CUMINJ(N-1) + INJN
CUMDSP(N) = CUMDSP(N-1) + DSP
C
C**** CALCULATE GAS REMAINING, MATERIAL BALANCE ERRORS, ETC.
430 POZAVG(N)=0.0
SM=0.0
DO 450 I=1,NR
PP=P(I)
CALL INTRP1(PT1,ZT,NT1,PP,ZZ)
Z(I)=ZZ
BG(I)=CON*Z(I)/P(I)
SM=SM+VP(I)/BG(I)
POZAVG(N)=POZAVG(N)+P(I)*VP(I)/Z(I)
450 CONTINUE
POZAVG(N)=POZAVG(N)*DRVOL
SMN=MCF1
IF(N.EQ.1)SMN=MCF1
MCF1=SM
NSC = SMN - MCF1
IMBE=NSC-PRCDN+INJN
MCF1=MCF1-CUMPRD(N)+CUMINJ(N)
MBE=(MCF1/MCF1 - 1.0) * 100.0
FGR=CUMPRD(N)/TGAS
IF(MCODE.EQ.0) GO TO 4702
C**** CHECK GAS INVENTORY
DO 480 I=2,NR
CUMI(I) = CUMI(I) + INJ(I)
CUMF(I) = CUMF(I) + PRD(I)
NSCM(I) = GMN(I) - GMCAL(I)
C
GMACT(I) = GASMI(I) - CUMF(I) + CUMI(I)
4800 CONTINUE
MCF1 = MCF1 - CUMINJ(N) + CUMDSP(N)
C

```

```

1CFDA = MCFDI - CUMDSP(N)
C
TGAS1 = MCFA + MCFMA + MCFDA
FGF = MCFA/TGAS1 *100.
FGM = MCFMA/TGAS1 *100.
FGD = MCFDA/TGAS1 *100.
C
FGGF = (MCFI-MCFA)/MCFI
FGGM = (MCFMI-MCFMA)/MCFMI
IF(MCFDI.NE.0.0) FGGD = (MCFDI-MCFDA)/MCFDI
IF(MCFDI.EQ.0.0) FGGD = 0.0
C
C
C*****PRINT NEW DISTRIBUTION & OTHER VALUES
4702 IF(N.NE.1.AND.N.NE.NMAX.AND.N.NE.KT) GO TO 998
PRINT 151,N,DELT,FT(N),TGAS,CUMPRD(N),FCZAVG(N),FCR,PRCN,INJ,N,DSP
&,NSC
&,IMBE,MCFA,MCFC,MJE,PW(N),SW(N)
C
PRINT 157,(IR(I),I=1,NR)
PRINT 155,(P(I),I=1,NR)
IF(MCODE.EQ.0) GO TO 998
PRINT 1571
DO 4500 I=2,NR
QM(N) = QM(N) + QSC(I)
QD(N) = QD(N) + QSCD(I)
PRINT 1575,I
DIFF = QSC(I) - QSCD(I)
PRINT 1573,(PM(I,J),J=1,NRM),QSC(I),QSCD(I),DIFF
4500 CONTINUE
PRINT 1577,QW(N),CM(N),QD(N)
C
DO 8700 I=2,NR
PRINT 4703,I
PRINT 4705,GASMI(I),PRD(I),INJ(I),NSCM(I),GMCAL(I)
C700 CONTINUE
C
C***** PRINT CURRENT GAS INVENTORY
PRINT 4117
PRINT 3119,MCFA,MCFMA,MCFDA
PRINT 4121,TGAS1,FGF,FGM,FGD
PRINT 4123,FGGF,FGGM,FGGD
C
C
998 IF(N.EQ.KT)KT=KT+KT1
1000 CONTINUE
GO TO 1005
1001 NN=N-1
GO TO 1010
1005 NN=N
1010 PRINT 163
DO 3002 N=1,NA
PRINT 165,N,FT(N),QW(N),PW(N),PWH(N),CUMPRD(N),FCZAVG(N)
3002 CONTINUE
1 FORMAT(15,15F5.0)
3 FORMAT(6(/),T15,'NUMBER OF RADIAL GRID-BLOCKS --- ',15)
5 FORMAT(///T15,'CUMULATIVE GRID-BLOCK RADII & CENTERS(FT)')
7 FORMAT(15X,15,2F15.4)
9 FORMAT(3F10.0)
11 FORMAT(///T15,'FORMATION THICKNESS(FT) = ',F6.1/)
13 FORMAT(15,7F10.0)
15 FORMAT(5(/),T15,'I-BLOCK PHI K(MD) P(PSIA)')
17 FORMAT(T15,15,F12.3,F14.6,F13.2)
1777 FORMAT(///T15,'MATRIX POROSITY & PERMEABILITY(FHIM,KLM) ARE: ',
&F12.4,&F15.6)
19 FORMAT(5(/),T15,'RADIUS OF CYLINDRICAL MATRIX ELEMENT(CM) = ',
&F6.1)
21 FORMAT(///T15,'CUMULATIVE GRID-BLOCK RADII(CM)')
23 FORMAT(15X,15,2F12.6)
51 FORMAT(15,F10.0)
69 FORMAT(40A2)
91 FORMAT(///T15,'RESERVOIR TEMPERATURE( DEG F) = ',F6.1//
& T15,'WELLHEAD TEMPERATURE( DEG F) = ',F6.1//
&, T15,'SHALE DENSITY(GRAMS/CC) = ',F6.3//
93 FORMAT(///T18,'GAS VISCOSITY & Z-FACTOR TABLE')
95 FORMAT(T15,' P(PSIA) MU(CP) 2')
97 FORMAT(13X,F10.2,F14.4,F15.3)
99 FORMAT(5(/),T15,'METHANE SORPTION ISOTHERM (AT RESERVOIR TEMP)')
101 FORMAT(T15,' P(ATM) CC AT STP/GM')
103 FORMAT(13X,F9.1,F12.3)
109 FORMAT(6X,' EV VP CUMVF', CUMMCF',
&' Z BG MCF CUMMCF',
&' MCFDI')
68

```

```

111 FORMAT(1X,14,8E15.6)
113 FORMAT(6X,'      BVM          VPM          RVCLM'//)
115 FORMAT(5(//),T15,'INITIAL GAS & PORE VOLUME -- FRACTURES'//)
117 FORMAT(5(//),T15,'INITIAL GAS & PORE VOLUME -- MATRIX'//)
125 FORMAT(F7.0,4X,4F8.0,5X,4F8.3)
127 FORMAT(1X,F10.2,5X,4F8.2,5X,4F8.2)
129 FORMAT(///T15,'BOTTOM-HOLE WELL PRESSURE HISTORY FOLLOWS'//)
131 FORMAT('      PWL          TIME CN (DAY,HR,MIN,SEC)
&' TIME OFF (DAY,HR,MIN,SEC)'//)
133 FORMAT(15,5F10.0,15)
135 FORMAT(///,
& T15,'MAXIMUM NUMBER OF TIME-STEPS          = ',14/
& T15,'MAXIMUM SIMULATION TIME(DAYS)         = ',F8.2/
& T15,'TIME-STEP CYCLE TOLERANCE(Psia)       = ',F8.3/
& T15,'MATRIX CYCLE TOLERANCE(Psia)         = ',F8.3/
& T15,'RESERVOIR PRESSURE TOLERANCE(Psia)    = ',F8.3/
& T15,'BACK PRESSURE EQUATION TOLERANCE(Psia) = ',F8.2/
& T15,'SKIP PRINT PARAMETER                 = ',15//)
137 FORMAT(8F10.0)
139 FORMAT(/,'      I      DR      VIS      Z',
&'      K      TR      GAMMA')
141 FORMAT(/,'      I      AZ      EZ      CZ',
&'      DZ      PG      P ')
143 FORMAT(/T15,'BOTTOM-HOLE WELL PRESSURE HAS BEEN SPECIFIED ',F8.2,
&' PSIA THIS TIME-STEP'//)
145 FORMAT(1X,8E15.6)
151 FORMAT(///T15,'NUMBER OF TIME-STEPS COMPLETED          = ',15/
& T15,'SIZE OF CURRENT TIME-STEP(DAYS)          = ',F15.6/
& T15,'TOTAL ELAPSED TIME(DAYS)                 = ',F15.6//
& T15,'INITIAL GAS IN PLACE(MCF)                = ',F15.6/
& T15,'CUMULATIVE PRODUCTION(MCF)              = ',F15.6/
& T15,'VOLUMETRIC AVERAGE F/Z                 = ',F15.6/
& T15,'FRACTIONAL GAS RECOVERY                 = ',F15.6//
& T15,'PRODUCTION THIS STEP(MCF)              = ',F15.6/
& T15,'INJECTION FROM MATRIX THIS STEP        = ',F15.6/
& T15,'DESORPTION INTO MATRIX THIS STEP       = ',F15.6/
& T15,'SYSTEM CHANGE THIS STEP(MCF)          = ',F15.6/
& T15,'INCREMENTAL ERROR THIS STEP(MCF)       = ',F15.6//
& T15,'ACTUAL FRACTURE GAS REMAINING(MCF)     = ',F15.6/
& T15,'CALCULATED FRACTURE GAS REMAINING     = ',F15.6/
& T15,'CUM. MATERIAL BALANCE ERROR(%)        = ',F15.6//
& T15,'BOTTOM-HOLE PRESSURE(Psia)            = ',F15.6/
& T15,'PRODUCTION RATE THIS STEP(MCFD)       = ',F15.6//)
155 FORMAT(//5X,16F7.1))
157 FORMAT(///T25,'**** RESERVOIR PRESSURE DISTRIBUTION ****'//,
&2X,18I7)
1571 FORMAT(///T10,'----- MATRIX PRESSURE DISTRIBUTIONS, SOURCE RATE'
&' , DESORPTION RATE, & FREE GAS RATE -----'//)
1573 FORMAT(1X,16F8.2)
1575 FORMAT(/T5,'RESERVOIR NODE ',13)
1577 FORMAT(///T15,'..... SUMMARY OF FLOW RATES THIS STEP',
&'(MCFD) .....'//T5,'WELL PRODUCTION RATE',
&T35,'RATE INTO FRACTURES',T70,'RATE OF DESORPTION',
&T5,'-----',T35,'-----',T70,
&'-----'//)
&T4,F12.3,T36,F12.3,T73,F12.3)
161 FORMAT(T2,'***** ENDING CYCLE ',12,4X,'FOR TIME-STEP',
&1X,14,4X,'DP = ',E11.4,4X,'P(1) = ',E11.4,3X,'P(2) = ',E11.4)
153 FORMAT(9(//),T15,'***** SUMMARY TABLE FOLLOWS *****',
&'//
&'      N      FT      G%      F%      PWH',
&'      CUMPRD      POZAVG'//)
165 FORMAT(1X,15,F15.6,F15.3,2F10.2,F15.3,F10.2)
167 FORMAT(///T15,'WELL PRODUCTION HISTORY FOLLOWS'//)
169 FORMAT('      G(MCFD)          TIME CN (DAY,HR,MIN,SEC)
&' TIME OFF (DAY,HR,MIN,SEC)'//)
171 FORMAT(/T15,'WELL PRODUCTION RATE HAS BEEN SPECIFIED AT ',F11.2,
&' MCFD THIS TIME-STEP'//)
175 FORMAT(///T15,'SKIN FACTOR IS SPECIFIED AT ',F5.2/
& T15,'PERMEABILITY OF NODE 2 HAS BEEN DECREASED TO ',
&F12.6,' MD'//)
177 FORMAT(///T15,'GAS GRAVITY, TUBING ID & ROUGHNESS(IN)',
&' , WELL DEPTH(FT) & DEFAULT VALUE FOR F : ',3F8.5,F8.2,F8.5//
&T15,'TUBING CD & CASING ID (IN) ARE: ',2F8.4//)
181 FORMAT(///T15,'PARAMETERS A1,A2,VWELL,TPI ARE : ',4E15.6//)
183 FORMAT(16I5)
195 FORMAT(///T15,'WELLHEAD PRESSURE HISTORY FOLLOWS'//)
187 FORMAT(/T5,'SPECIFIED WELLHEAD PRESSURE IS ',F8.2,' PSIA ',
&6X,'CALCULATED BOTTOM-HOLE PRESSURE IS ',F8.2)
189 FORMAT(T5,'(QAV,RE,F,IF,PBH2,ILHF) = ',3E15.6,110,E15.6,110)
191 FORMAT(/T15,'WELLBORE STORAGE OPTION IS IN EFFECT WHEN NEITHER ',
&'RATE NOR PRESSURE IS SPECIFIED'//)
193 FORMAT(///T15,'EACK PRESSURE OPTION IS IN EFFECT WHEN PRESSURE ',
&'HISTORY IS SPECIFIED')
195 FORMAT(///T15,'WELL HAS BEEN SHUT-IN & STORAGE OPTION IS CN',

```



```

SUBROUTINE INTERP1(X,Y,N,X0,Y0)
IMPLICIT REAL*8 (A-H,O-Z)
DIMENSION X(1),Y(1)
IF(X0.EQ.X(N))Y0=Y(N)
IF(X0.EQ.X(1))RETURN
DO 1) I=2,N
IF(X0.GE.X(I))GO TO 10
Y0=Y(I-1)+(X0-X(I-1))*(Y(I)-Y(I-1))/(X(I)-X(I-1))
RETURN
CONTINUE
END
10

```

```

SUBROUTINE TRNRQ(NR,P,TR,K,DR,Z,V,TPI)
IMPLICIT REAL*8 (A-H,O-Z)
REAL*8 K(1)
DIMENSION TR(1),DR(1),Z(1),V(1),F(1)
IF(NR.EQ.1)GO TO 601
DO 75 I=2,NR
TR(I)=TPI * (P(I-1)+P(I)) * K(I-1) * K(I)/
&(K(I) * V(I-1) * Z(I-1) * DLOG(2.*DR(I)/(DR(I-1)+DR(I))) +
&K(I-1) * V(I) * Z(I) * DLOG((DR(I)+DR(I+1))/(2.*DR(I))))
CONTINUE
75
601 CONTINUE
RETURN
END

```

```

SUBROUTINE LTRI(N,AZ,BZ,CZ,DZ,EZ,FZ,UZ)
IMPLICIT REAL*8 (A-H,O-Z)
C
C THIS PROGRAM SOLVES THE TRIDIAGONAL SYSTEM
C GENERATED BY THE SYSTEM OF N EQUATIONS
C
C  $A(I)*P(I-1) + E(I)*U(I) + C(I)*P(I+1) = D(I)$ 
C
C WITH  $A(1)=C(N) = 0.0$ 
C
DIMENSION AZ(1),EZ(1),CZ(1),DZ(1),EZ(1),FZ(1),UZ(1)
BB=1./BZ(1)
EZ(2)=-CZ(1)*BB
FZ(2)= DZ(1)*BB
DO 1) I=2,N
FF=1./(AZ(I)*EZ(I)+BZ(I))
EZ(I+1)=-CZ(I)*FF
10 FZ(I+1)=(DZ(I)-AZ(I)*FZ(I))*FF
UZ(N)=FZ(N+1)
K=N
NN=N-1
DO 2) I=1,NN
K=K-1
20 UZ(K)=EZ(K+1)*UZ(K+1) + FZ(K+1)
RETURN
END

```

```

SUBROUTINE FRIC(G,G,V,D,E,P,F,D,DFTV),
  IMPLICIT REAL*8 (A-H,O-Z)
C
C**** ROUTINE FOR CALCULATING FRICTION FACTOR FOR PIPE FLOW
C---- FOR LAMINAR FLOW OR TRANSITION OR TURBULENT FLOW ----
C
C**** REFERENCE --- "HANDBOOK OF NATURAL GAS ENGINEERING" BY KATZ
C
C F = 64/RE FOR LAMINAR FLOW (1000<RE<2100)
C F = IMPLICIT FUNCTION (EQ. (7-25) OF KATZ) FOR TRANSITION OR
C TURBULENT FLOW
C
C NEWTON-RAPHSON METHOD USED FOR IMPLICIT FUNCTION
C
C A DEFAULT VALUE USED IF RE IS IN THE CRITICAL ZONE
C
C ALSO THE DEFAULT VALUE IS USED IF THE NEWTON-RAPHSON SCHEME
C DOES NOT CONVERGE
C
C Q = RATE --- MCFD
C G = GAS GRAVITY
C V = VISCOSITY --- CP
C D = PIPE ID --- IN
C E = ABSOLUTE ROUGHNESS --- IN
C R = REYNOLDS NUMBER
C F = FRICTION FACTOR (TO BE CALCULATED & RETURNED)
C I = NUMBER OF ITERATIONS TO CONVERGENCE
C DFTV = DEFAULT VALUE (USED FOR CRITICAL ZONE)
C
F=0.0
ICRIT=0
A=D/E
R=20. * Q*G/(V*D)
I=0
IF(R.LT.1000) RETURN
C**** F=64/RE NOT VALID FOR VERY LOW FLOW RATES BEFORE LAMINAR FLOW IS
C ESTABLISHED; VALUE OF F RETURNED IN THIS CASE IS 0.0
C
IF(R.LE.2100.)F=64./R
IF(R.LE.2100.)RETURN
C
IF(R.GT.2100. .AND. R.LE. 4000.) GO TO 20
C
C=9.34*A/R
C
C**** USE KATZ EQ (7-25) WHICH IS FIRST TERM OF IMPLICIT FN AS INITIAL GUESS
X=2.*DLOG10(A) + 1.14
2 FN = X - 2.0 * (DLOG10(A/(1.+C*X)) + 0.57)
IF(DABS(FN).LE.1.E-6) GO TO 3
DC=1./C
DFDX = 1. + .8686/(DC + X)
X = X - FN/DFDX
I=I+1
IF(I.GT.99)PRINT 5,I,X,FN,DFDX
IF(I.GT.99) GO TO 10
GO TO 2
3 F=1./(X*X)
RETURN
C
5 FORMAT(////T2,'(ITER, X, FN, DFDX) ',I3,3E15.6)
7 FORMAT(////T5,'REYNOLDS NUMBER IS IN CRITICAL RANGE -- ',F6.0,
6 /T5,'THEREFORE DEFAULT VALUE OF -- ',F8.4,' IS BEING USED')
10 F=DFTV
RETURN
12 F=DFTV
PRINT 7,R,DFTV
RETURN
END

```

```

SUBROUTINE PBH(A1,A2,Q,F,PBH1,PWH,DPW,PT1,ZT,NT1,PBH2,ZAV,PAV,I)
IMPLICIT REAL*8 (A-H,O-Z)
DIMENSION PT1(1),ZT(1)
H(X,Z)=(DEXP(X/Z) - 1.) * Z#Z/X
C
C**** PWH = FIXED WELLHEAD PRESSURE
C      PBH1 IS STARTING VALUE OF BOTTOM-HOLE PRESSURE
C      NOTE THAT ITERATION IS ONLY ON Z; HOWEVER, ANY TIME BHP OR
C      Q CHANGES IT IS NECESSARY TO REFORM THE ITERATIVE PROCEDURE
C
      I=0
      PAV=0.5*(PWH+PBH1)
      CALL INTRP1(PT1,ZT,NT1,PAV,ZAV)
C
      PBH2 = DSORT(DEXP(A2/ZAV)*PWH*PWH + A1*H(A2,ZAV)*F*Q*Q)
      DPPW=PBH2-PBH1
      I=I+1
      IF(I.GT.99)PRINT 7,PAV,ZAV,PBH2,DPPW
      IF(I.GT.99)RETURN
C
      IF(DABS(DPPW).LT.DPW) RETURN
C
      PBH1=PBH2
      GO TO 1
C
7     FORMAT(//T5,'BOTTOM-HOLE PRESSURE ROUTINE WILL NOT CONVERGE'/
&T5,'PAV, ZAV, PBH2, DPPW ',3X,4E15.6/)
C
      RETURN
      END

```

```

SUBROUTINE NLLSCS(MCCEFF,NPTS,X,Y,A,B,C,FF,E,YE,DEV,PCTDEV,FP)
IMPLICIT REAL*8 (A-H,O-Z)
DIMENSION X(1),Y(1),A(MCCEFF,1),E(1),C(1),FF(MCCEFF,1),E(1),
&YE(1),DEV(1),PCTDEV(1),FP(1)
C
C LEAST SQUARES PROGRAM - APPROXIMATING FUNCTION NON-LINEAR
C IN ITS COEFFICIENTS:  $Y = A*X/(1 + B*X)$ 
C  $F(X,B1,B2)=B1*X/(1. + B2*X)$ 
C
C INSERT ARITHMETIC STATEMENT FUNCTIONS DESCRIBING THE PARTIALS OF
C F WITH RESPECT TO EACH OF B1,B2,....,MCCEFF.
C  $F1(X,B1,B2)=X/(1.+ B2*X)$ 
C  $F2(X,B1,B2)=-B1*X*X/((1.+B2*X)**2)$ 
C
C  $DFDX(X,B1,B2)= B1/( (1.+B2*X) *(1.+B2*X) )$ 
C
C PRINT INITIAL ESTIMATES OF THE COEFFICIENTS TO BE DETERMINED
PRINT 1031,B(1),B(2)
1031 FORMAT(/T15,'INITIAL ESTIMATES OF COEFFICIENTS B1 & B2 ARE: ',
&2E15.6/)
C
C KTR=0
C
C BUILD MATRIX FF BY LETTING FF(I,J)=FI(X(J),E(1),E(2),...,B(MCCEFF))
C I=1,2,...,MCCEFF
10 BB1=B(1)
BB2=B(2)
DO 1 J=1,NPTS
XX=X(J)
FF(1,J)=F1(XX,BB1,BB2)
FF(2,J)=F2(XX,BB1,BB2)
1
C
C BUILD MATRIX A, TAKING ADVANTAGE OF SYMMETRY WITH RESPECT TO
C MAIN DIAGONAL
DO 3 I=1,MCCEFF
DO 3 K=1,I
A(K,I)=0.
DO 2 J=1,NPTS
2 A(K,I)=A(K,I)+FF(I,J)*FF(K,J)
3 A(I,K) = A(K,I)
C
C BUILD MATRIX C
DO 4 K=1,MCCEFF
C(K) = 0.0
DO 4 J=1,NPTS
XX=X(J)
4 C(K)=C(K)+(Y(J)-F(XX,BB1,BB2))*FF(K,J)
9000 FORMAT(1X,7E15.6)
C
C**** SOLVE THE SYSTEM OF EQUATIONS AE = C
E(1) = (C(1)-A(1,2)*C(2)/A(2,2))*X(A(1,1)-A(1,2)*A(2,1)/A(2,2))
E(2) = (C(1)-A(1,1)*E(1))/A(1,2)
C
C ERR=0.0
KTR=KTR+1
C
C MAKE CORRECTIONS TO ESTIMATES OF COEFFICIENTS
DO 5 I=1,MCCEFF
B(I)=B(I)+E(I)
5 ERR=ERR+DAFS(E(I))
C
C IS SUM OF CORRECTIONS TO COEFFICIENTS SMALL ENOUGH
IF(ERR.GT..1.AND.KTR.LT.25)GO TO 10
IF(KTR.NE.25)GO TO 9
C
C IF AFTER 25 TRIALS SUM OF CORRECTIONS IS STILL TOO LARGE, STOP
WRITE(6,105)
105 FORMAT(43HNON-LINEAR LEAST SQUARES FAILED TO CONVERGE)
STOP

```

```

C
C   IF CONVERGENCE HAS BEEN REACHED, PRINT OUT THE COEFFICIENTS
9   B1=E(1)
   B2=E(2)
   PRINT 119,B1,B2
C
   PCTDEV(1)=0.0
   DO 90 J=1,NPTS
   XX=X(J)
   YE(J)=F(XX,B1,B2)
   DEV(J)=YE(J)-Y(J)
   IF(J.GT.1)PCTDEV(J)=DEV(J)/Y(J) * 100.0
   FP(J)=DFDX(XX,B1,B2)
90  CONTINUE
   PRINT 107
   PRINT 123,(X(J),Y(J),YE(J),DEV(J),PCTDEV(J),FP(J),J=1,NPTS)
119  FORMAT(/T5,'NON-LINEAR LEAST SQUARES COEFFICIENTS TO EQUATION',
&' C = AP/(1 + BP) ARE AS FOLLOWS'/,T15,'A = ',E12.6,5X,
&' B = ',E12.6/)
107  FORMAT(T15,'      P(PSIA)      SCF/CU FT      EST VALUE      DEV%',
&'      PCTDEV      DCDP')
123  FORMAT(16X,F9.1,F12.3,F12.3,F15.6,F10.2,E15.6)
   RETURN
   END

```

TABLE 1 -- MODEL INPUT DATA FOR SENSITIVITY ANALYSIS

| | <u>Minimum Value</u> | <u>Base Case</u> | <u>Maximum Value</u> |
|-----------------------------|---------------------------|---|--------------------------|
| Wellbore Radius | --- | 0.3 ft. | --- |
| Drainage Radius | 500 ft. | 933 ft. | 2,000 ft. |
| Reservoir Temperature | --- | 100 ^c F | --- |
| Initial Reservoir Pressure | --- | 500 psia | --- |
| Wellbore Flowing Pressure | --- | 200 psia for 4 years/ 50 psia for 26 years | --- |
| Specific Gravity of Gas | --- | 0.60 | --- |
| Shale Bulk Density | --- | 2.60 g/cm ³ | --- |
| Gas Viscosity | --- | 0.0115 cp | --- |
| Formation Thickness | --- | 500 ft. | --- |
| Formation Depth | --- | 3,720 ft. | --- |
| Fracture Porosity | 0.0025 | 0.005 | 0.01 |
| Fracture Permeability | 0.05 md | 0.10 md | 0.2 md |
| Shale Matrix Porosity | 0.02 | 0.06 | 0.10 |
| Shale Matrix Permeability | 0.69×10^{-10} md | 0.69×10^{-9} md | 0.69×10^{-8} md |
| Shale Matrix Element Radius | 5 cm | 25 cm | 50 cm |
| Klinkenberg Factor | 0 | $b = 12.64 \text{ km}^{-.33}$ | --- |
| Total Simulation Time | --- | 30 years | --- |

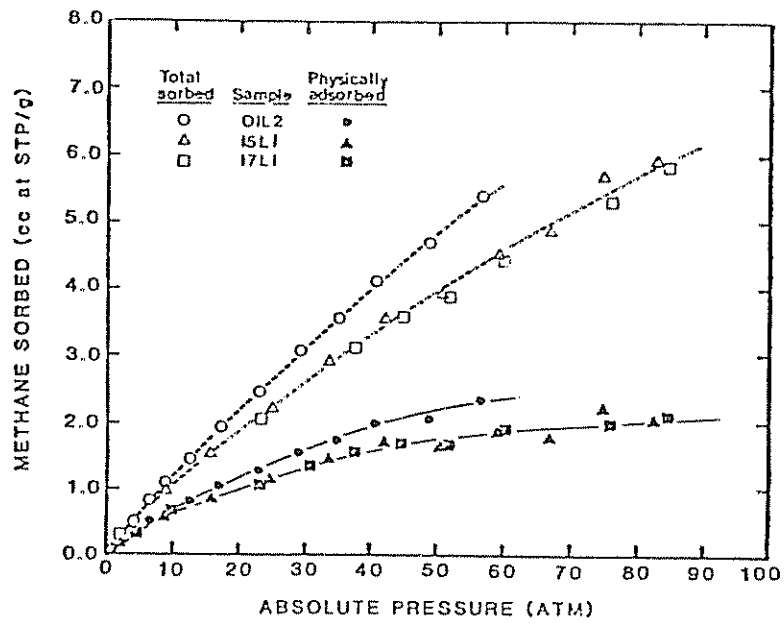


Fig. 1 - Methane Sorption Isotherms at 28°C

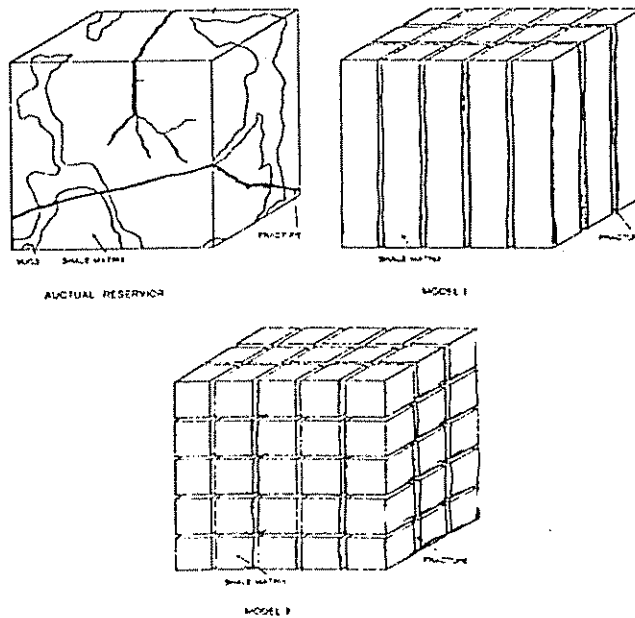


Fig. 2 - Fractured Devonian Shale Reservoir Systems

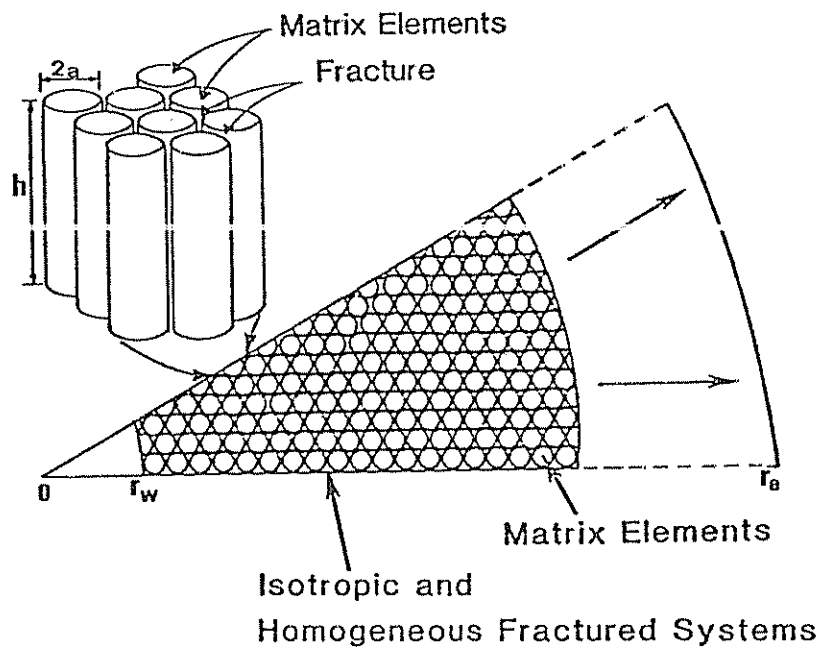


Fig. 3 - Radial One-Dimensional Devonian Shale Reservoir Model

$$\bar{r}_i = \frac{1}{2}(r_{i+1} + r_i)$$

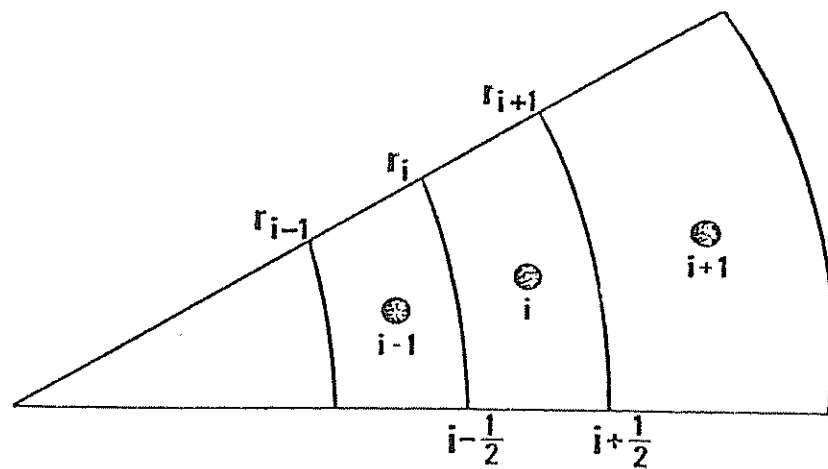


Fig. 4 - Reservoir Finite-Difference Grid System

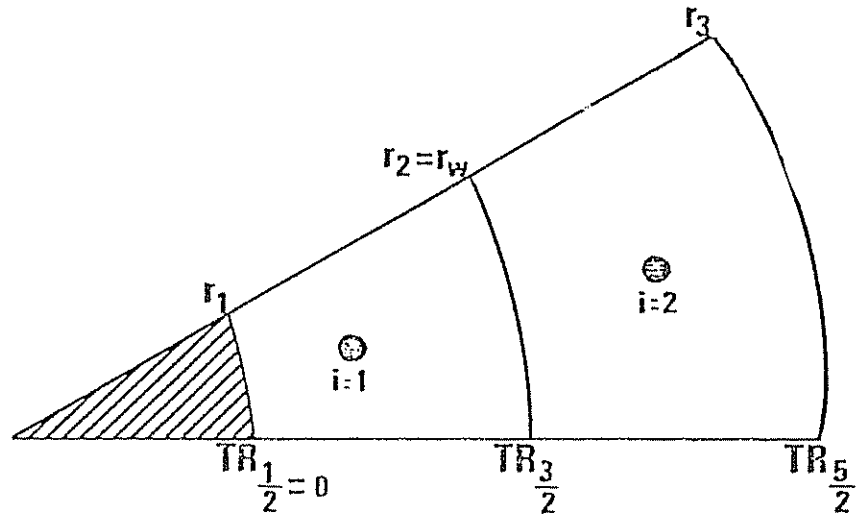


Fig. 5 - Block-Centered Finite-Difference Scheme at the Wellbore

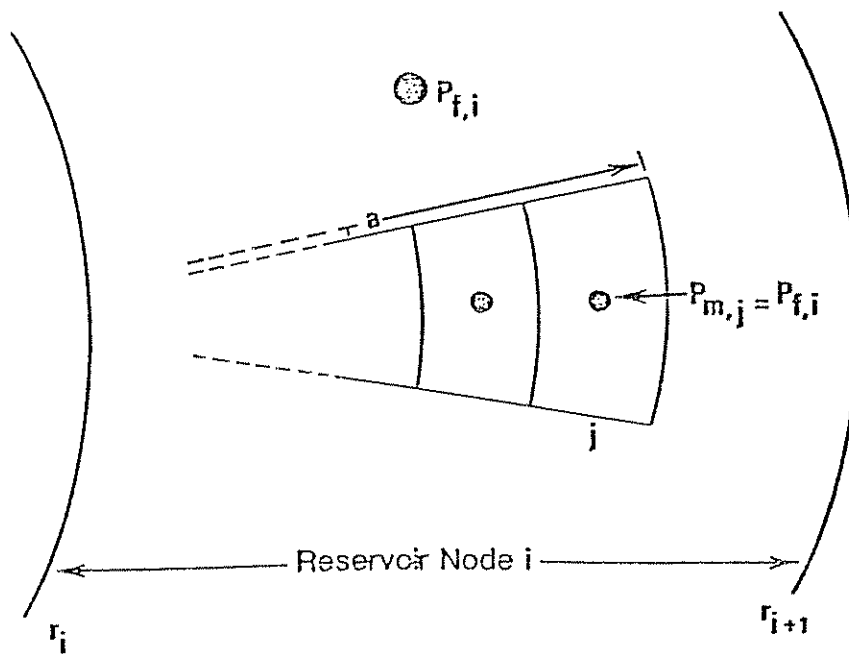


Fig. 6 - Matrix Element Finite-Difference Scheme

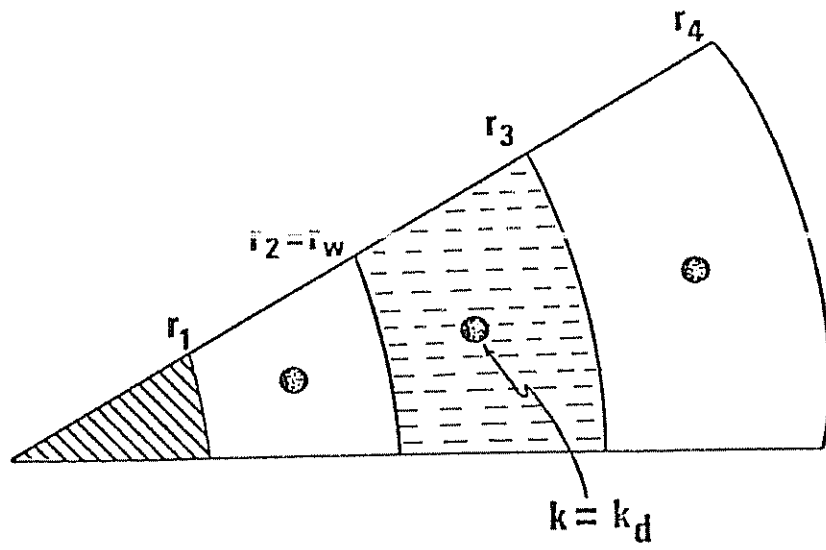


Fig. 7 - Damaged Zone in Finite-Difference Scheme

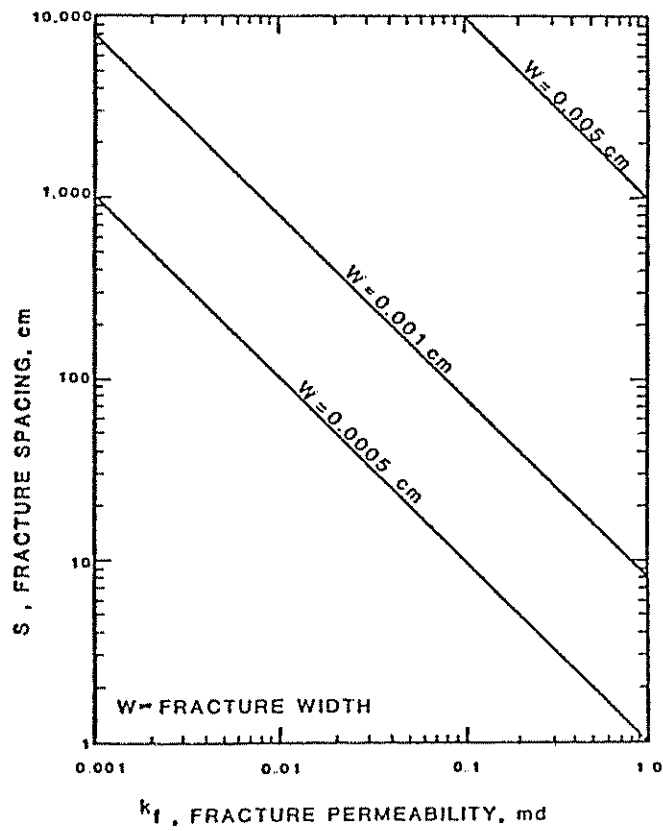


Fig. 8 - Fracture Permeability versus Fracture Spacing for Various Fracture Width

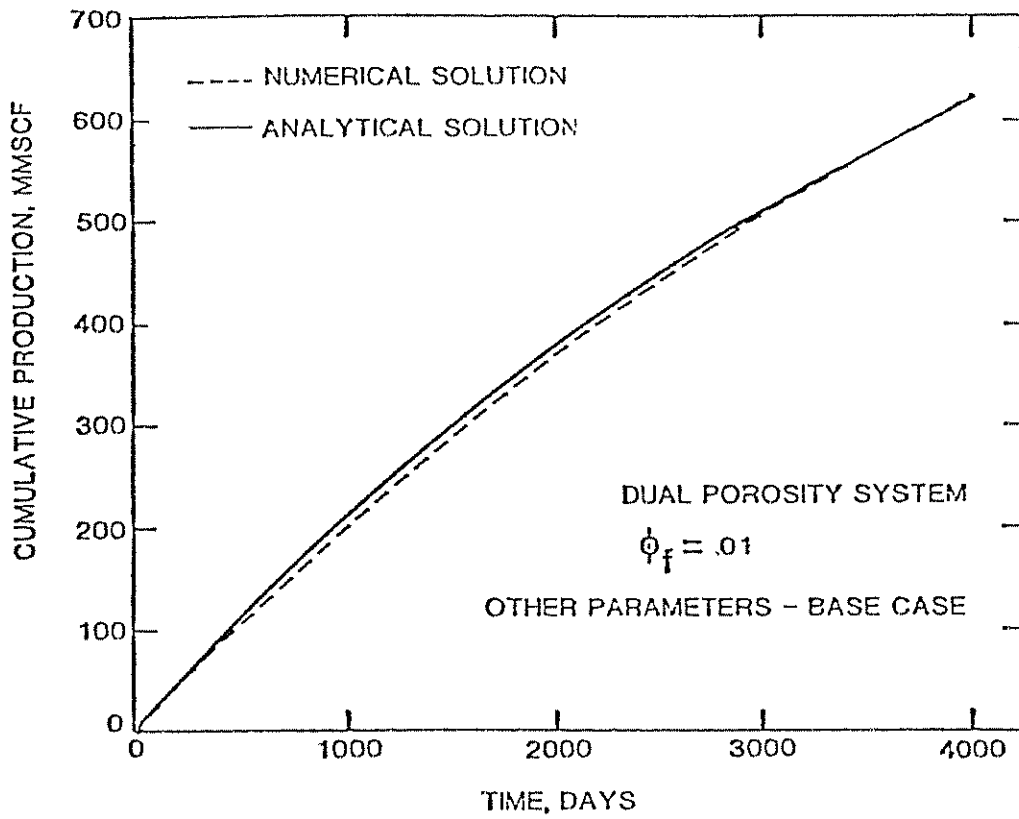


Fig. 9 - Comparison of Numerical and Analytical Solutions

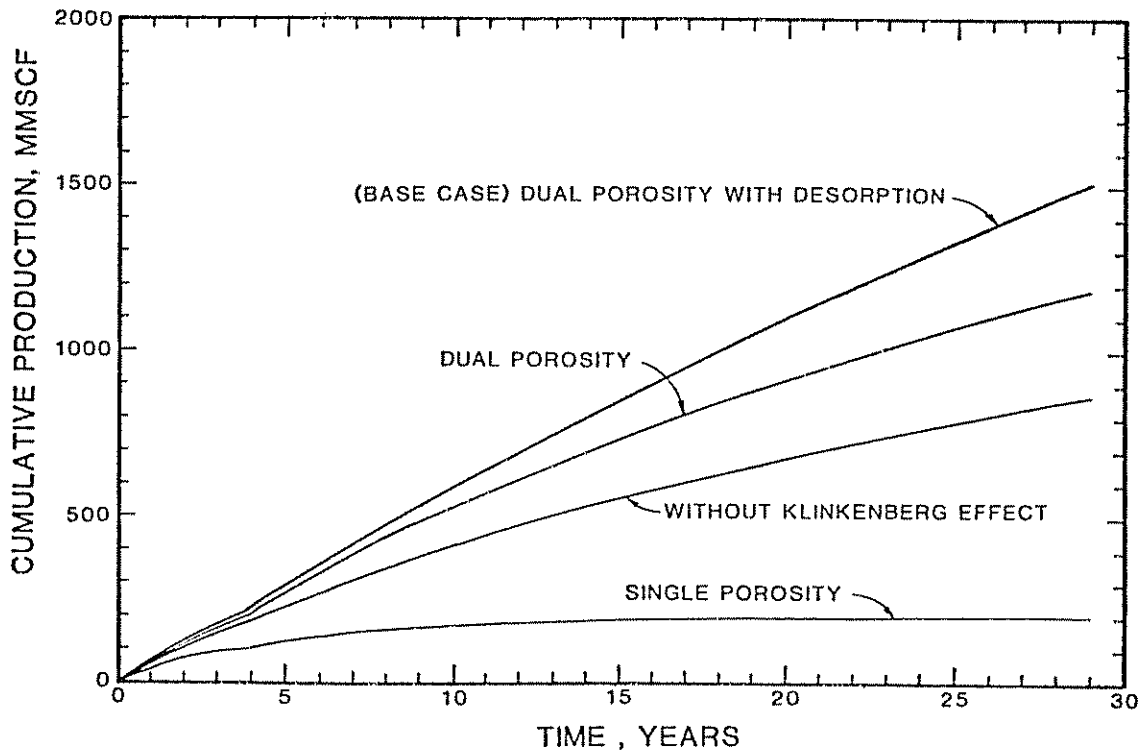


Fig. 10 - Productivity Improvement with Dual Porosity and Desorption

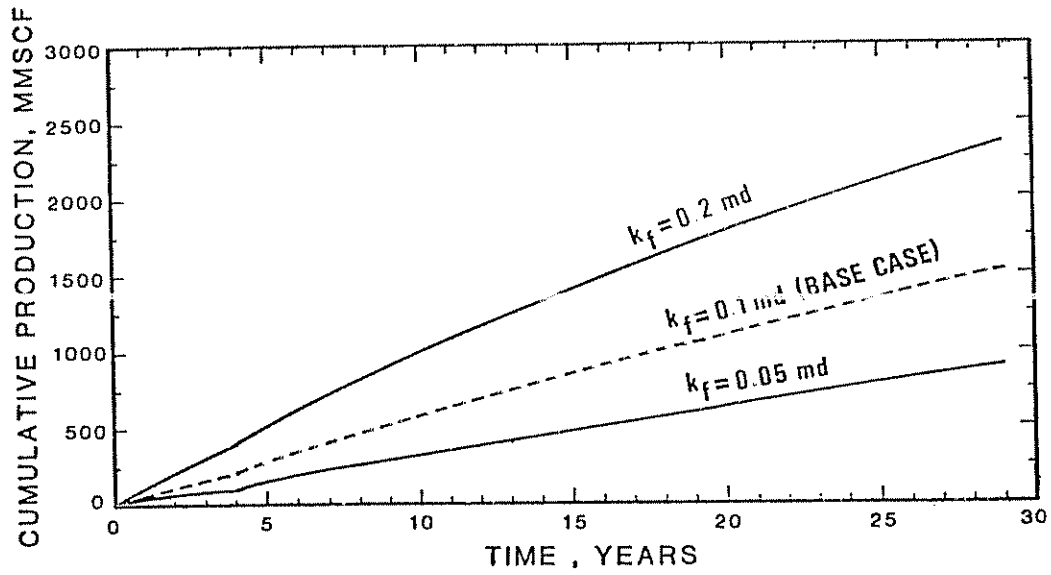


Fig. 11 - Effect of Fracture Permeability on Cumulative Production

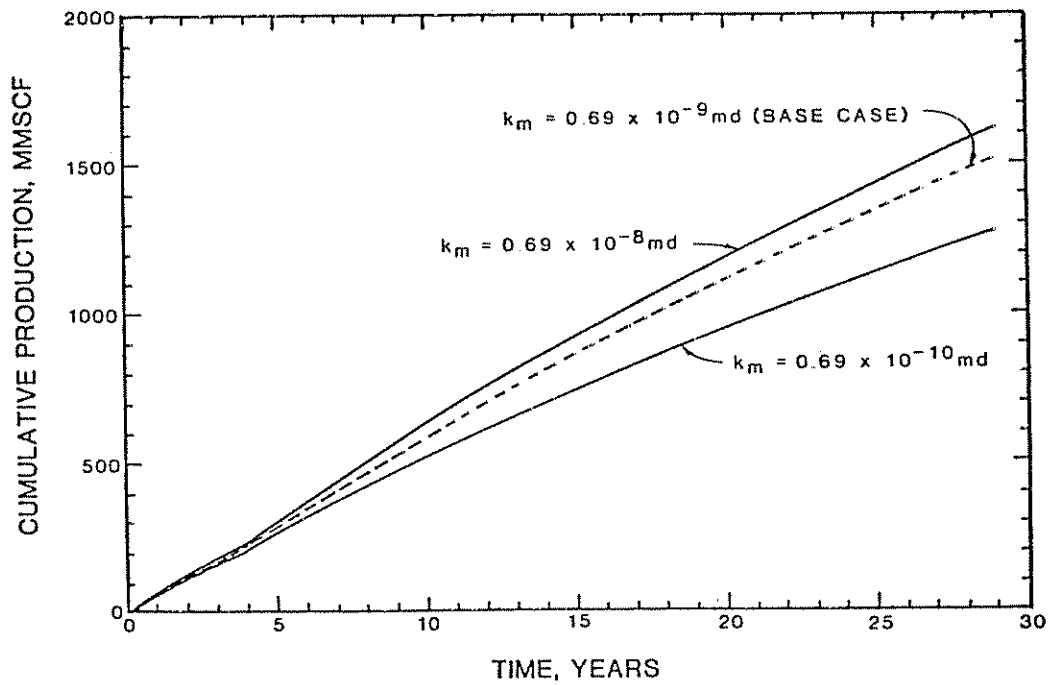


Fig. 12 - Cumulative Production as a Function of Time for Various Matrix Permeability

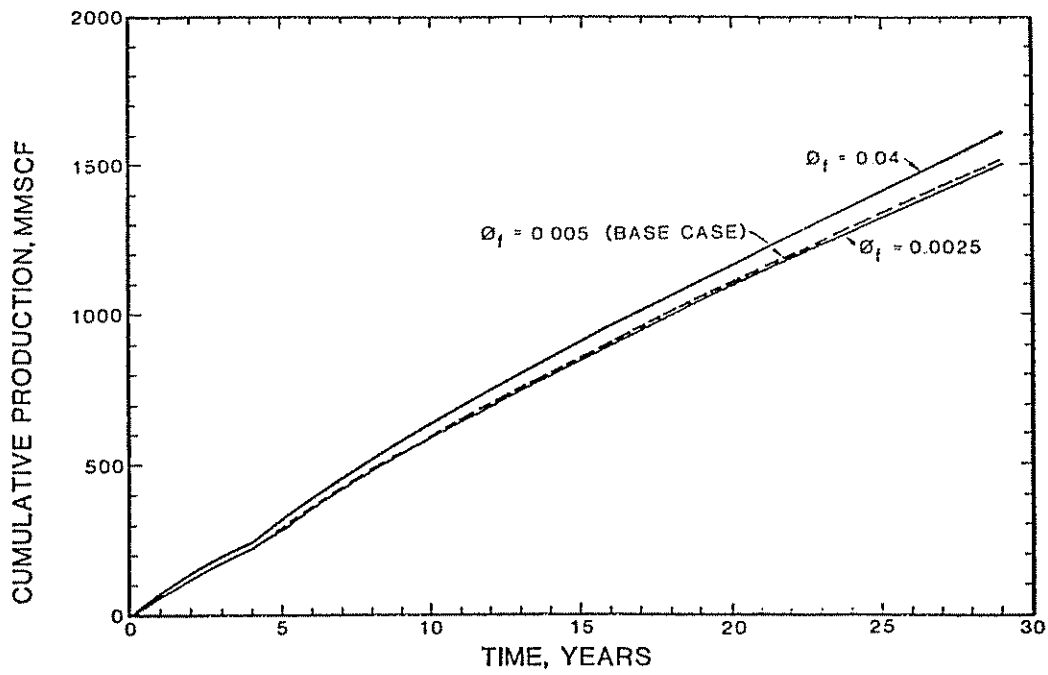


Fig. 13 - Effects of Fracture Porosity on Cumulative Production

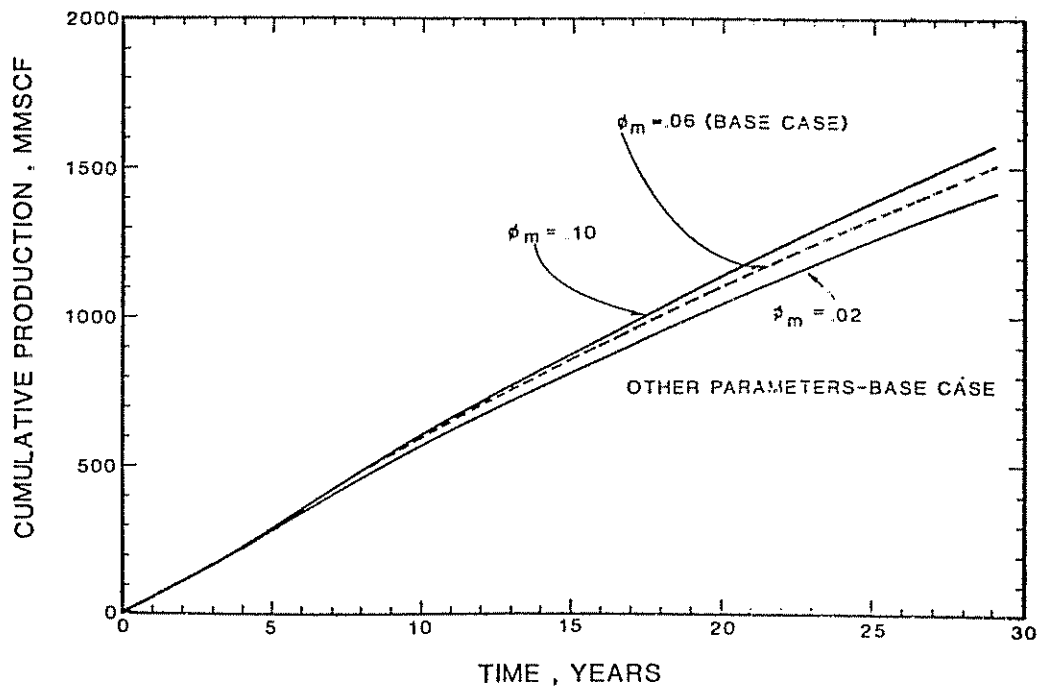


Fig. 14 - Effects of Matrix Porosity on Cumulative Production

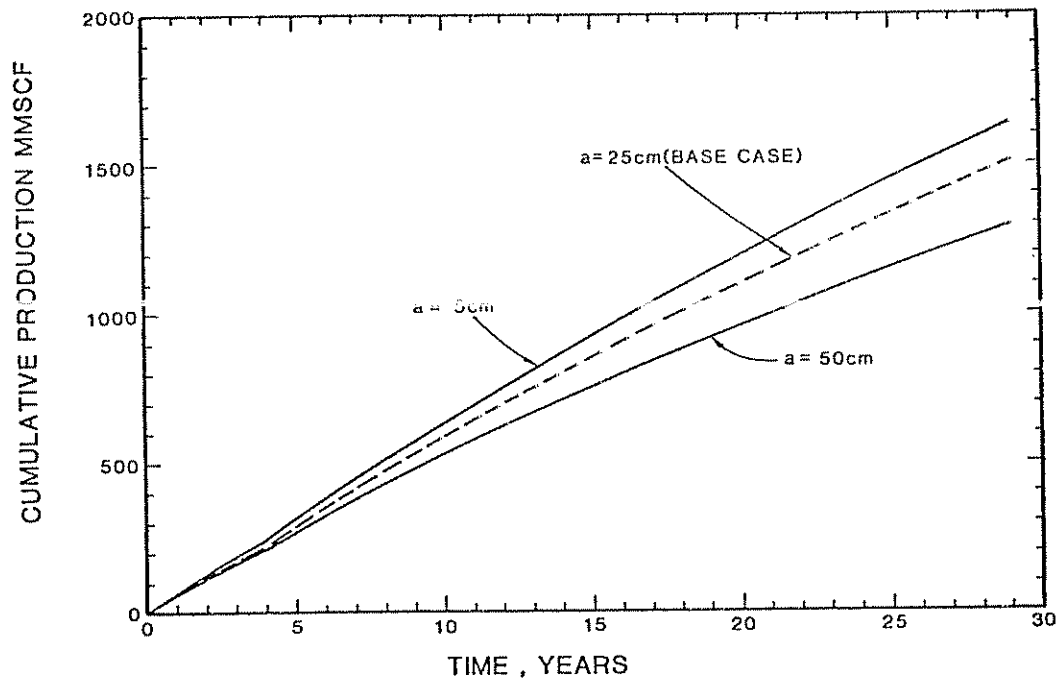


Fig. 15 - Comparison of Cumulative Production for Different Matrix Element Sizes

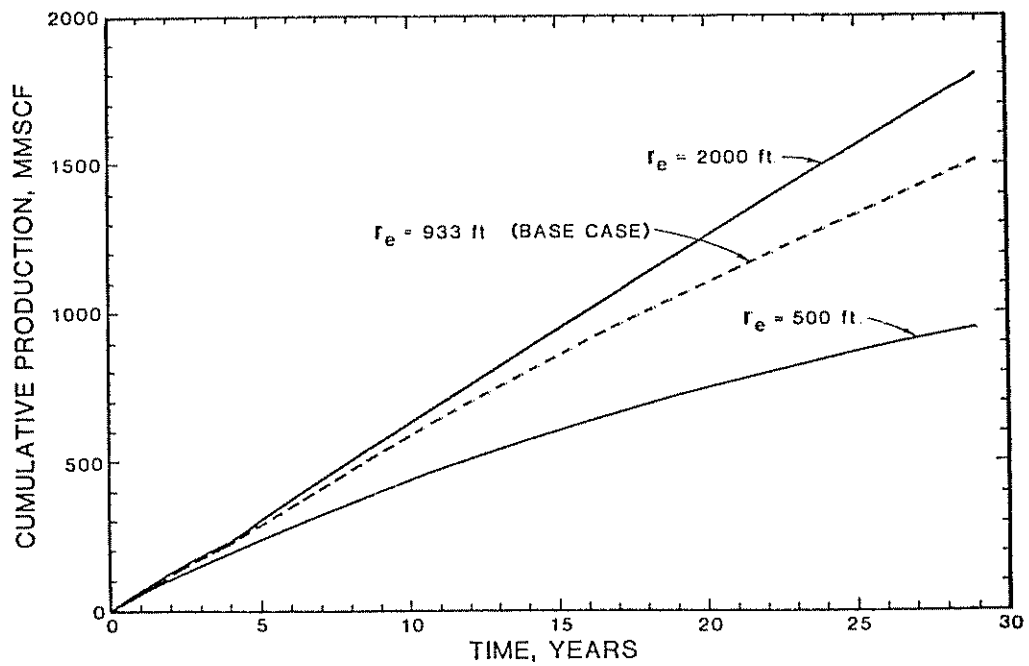


Fig. 16 - Cumulative Production for Different Drainage Radii

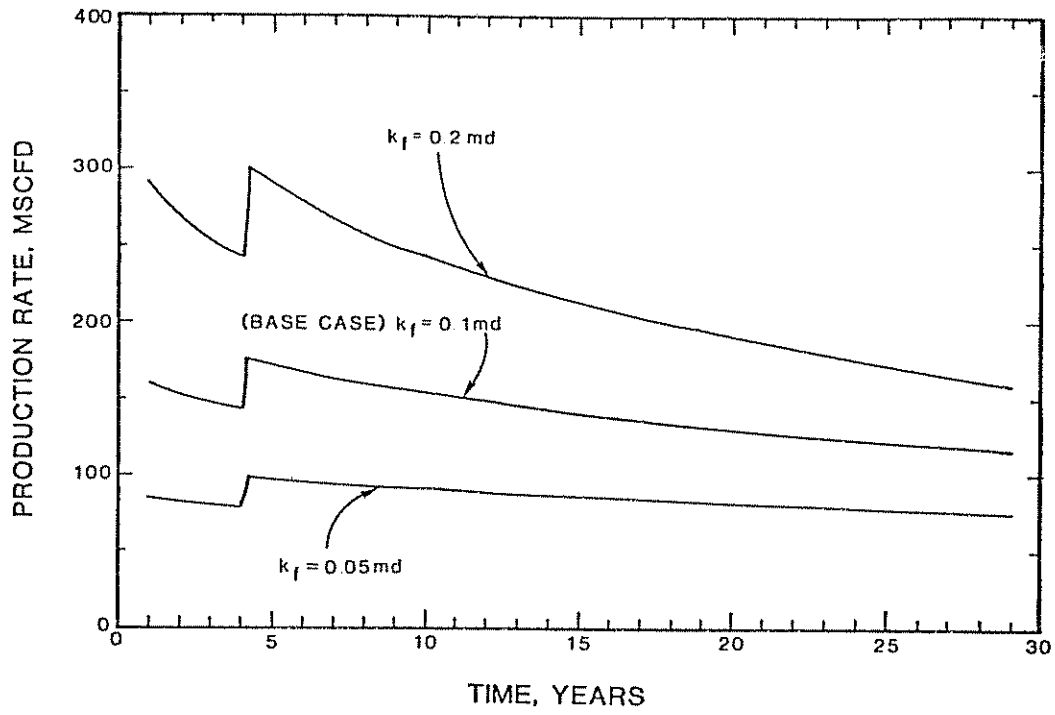


Fig. 17 - Production Rate for Different Fracture Permeabilities

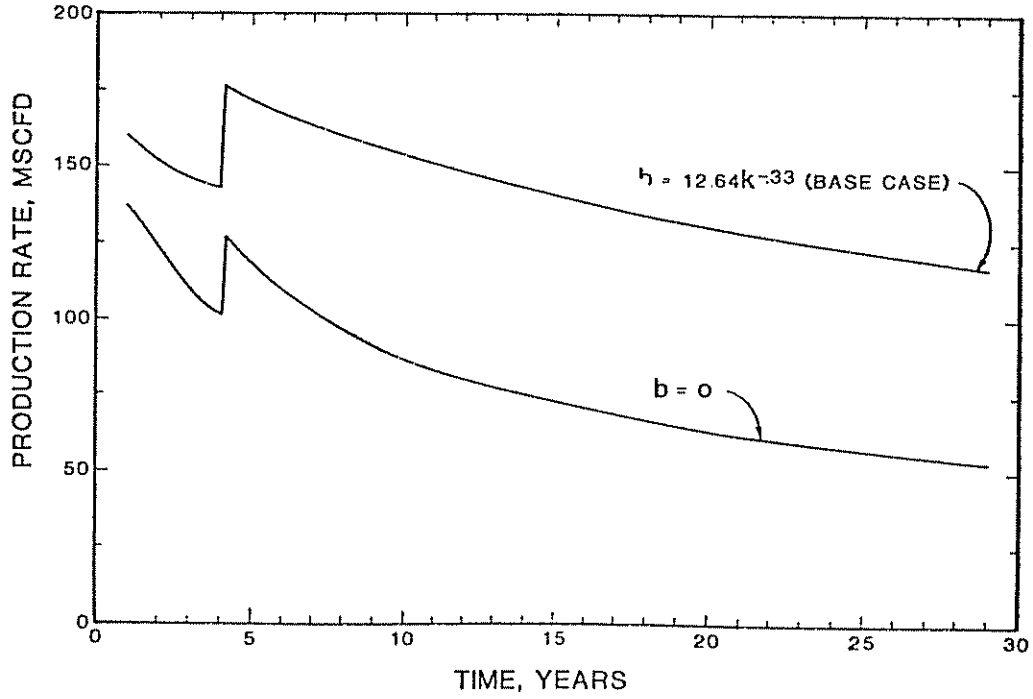


Fig. 18 - Effect of Gas Slippage on Production Rate

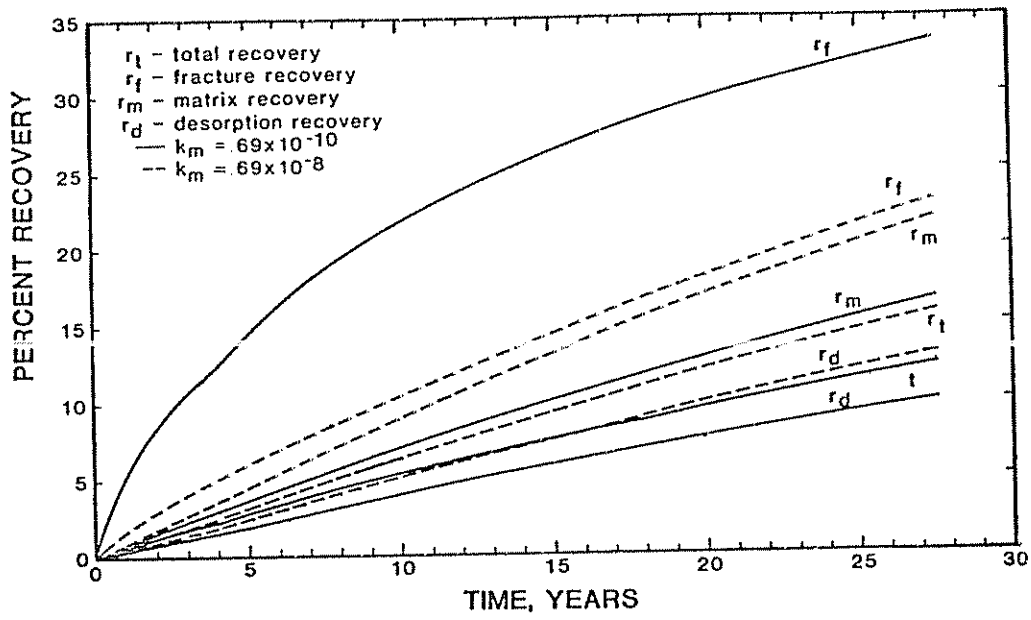


Fig. 19 - Breakdown of Resource Recovery

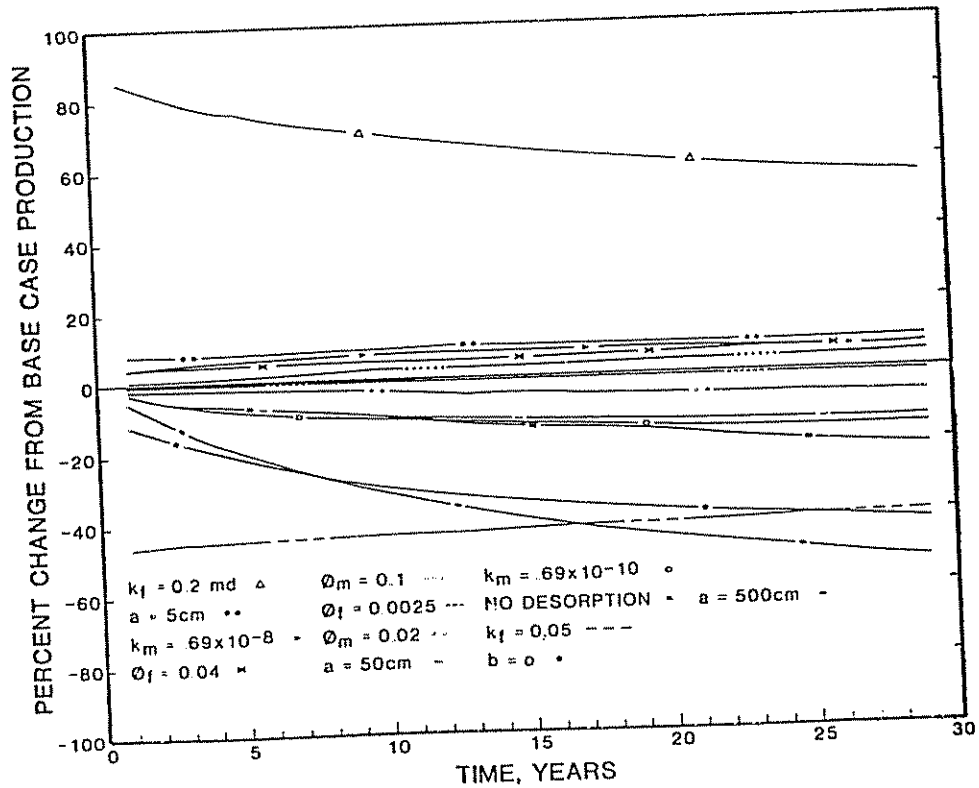


Fig. 20 - Sensitivity of Various Parameters on Cumulative Production

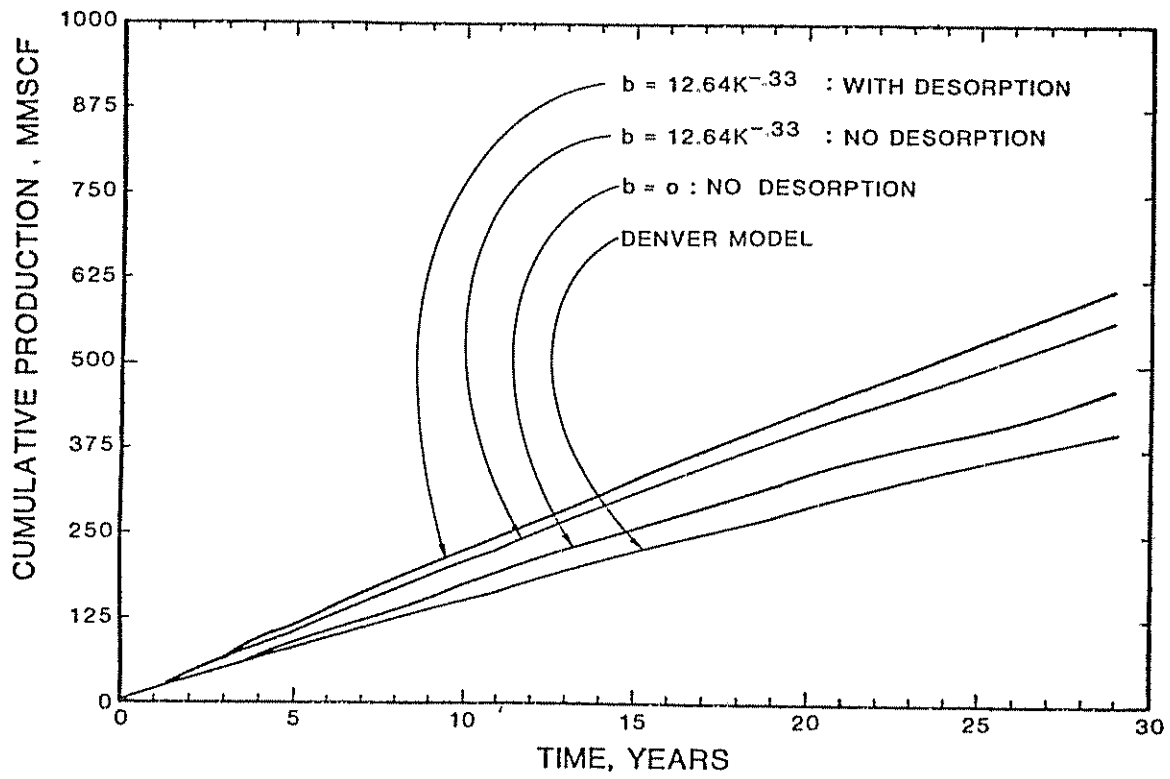


Fig. 21 - Comparison of Cumulative Production Using Different Models

